A. A LIQUID HELIUM STAGE FOR THE PHILIPS E.M. 300 ELECTRON MICROSCOPE

B. A STUDY OF FACE-CENTRED-CUBIC THIN FILMS OF SOME RARE-EARTH METALS AND THEIR OXIDES

by

Herbert Gustav Chlebek

B.Sc., Simon Fraser University, 1971

A THESIS SUBMITTED IN PARTIAL FULFILLMENT OF THE REQUIREMENTS FOR THE DEGREE OF

MASTER OF SCIENCE

in the Department

of

Physics

SIMON FRASER UNIVERSITY

December 1973

APPROVAL

Name: Herbert Gustav Chlebek

Degree: Master of Science

Title of Thesis: Part A: A Liquid Helium Stage for the Philips E.M. 300 Electron Microscope.
Part B: A Study of Face-Centred-Cubic Thin Films of Rare-Earth Metals and Their Oxides.

Examining Committee:

Chairman: Dr. K. S. Viswanathan

Dr. A. E. Curzon
Senior Supervisor

Dr. R. F. Frindt

Dr. E. D. Crozier

Dr. F. Einstein
Associate Professor
Department of Chemistry

Date Approved: December 7, 1973

PARTIAL COPYRIGHT LICENSE

I hereby grant to Simon Fraser University the right to lend my thesis or dissertation (the title of which is shown below) to users of the Simon Fraser University Library, and to make partial or single copies only for such users or in response to a request from the library of any other university, or other educational institution, on its own behalf or for one of its users. I further agree that permission for multiple copying of this thesis for scholarly purposes may be granted by me or the Dean of Graduate Studies. It is understood that copying or publication of this thesis for financial gain shall not be allowed without my written permission.

Title of Thesis/Dissertation:

A. A Liquid Helium Stage for the Philips E.M. 300 Electron Microscope;

B. A Study of Face-Centred-Cubic Thin Films of some Rare-Earth Metals and their Oxides.

Author: Mr. Herbert G. Chlebek

(signature)

(name)

Dec 19, 1973

(date)

ABSTRACT

Part A of this thesis describes a liquid helium stage for the Philips E.M. 300 electron microscope. The stage which makes use of an external reservoir for liquid helium enables a temperature of less than 9°K to be obtained at the specimen with a resolution of 60 Å. Helium consumption of the stage is relatively low at 1.4 litres per hour.

Part B describes high energy transmission electron diffraction and microscope studies of the following rare-earth metals, Gd, Tb, Dy, Ho, Er and Tm, the films being made by means of vapour deposition.

Films less than 200 Å thick had face-centred-cubic structures whereas in the thicker films the hexagonal-close-packed structures of the metals in bulk were observed.

Arguments are presented which indicate that the f.c.c. phase is the metal itself and not a chemical compound which occurs because of contamination of the film. For the case of erbium, experiments performed involving electrical conductivity and the weight increase which occurs when this phase is oxidized to Er_2O_3 shows that the phase is a new form of metallic erbium and is not ErO as suggested by another worker.

The lattice parameters of the face-centred-cubic forms of Gd, Tb, Dy, Ho, Er and Tm were found respectively to be 5.40, 5.20, 5.18, 5.15, 5.05 and 5.06 Å, the error being approximately $\pm$ 1%.

Oxidation of the films was observed in the vacuum in which they were deposited and also under the influence of the electron beam of the electron microscope. Arguments are presented to show that the space group of Er_2O_3 has T_h^7 symmetry and not T^5 as suggested by another author. A comment is made which casts doubt on the validity of recent electron microscope observations of gadolinium monoxide and a related lower oxide carried out by other workers.

ACKNOWLEDGEMENTS

I am indebted to Dr. A. E. Curzon for his encouragement and guidance throughout the entire research period and for his assistance in the writing of this thesis. I wish to thank Dr. E. D. Crozier and Dr. R. F. Frindt for their critical reading of the manuscript. Thanks are due also to Mr. Frank Wick and his machinists for the construction of the helium stage. The financial support of the National Research Council of Canada and the Simon Fraser University Physics Department is gratefully acknowledged.

TABLE OF CONTENTS

LIST OF TABLES

PART B

LIST OF FIGURES

PART A

PART B

PART A. A LIQUID HELIUM STAGE FOR THE PHILIPS E.M. 300 ELECTRON MICROSCOPE

CHAPTER I

INTRODUCTION

Electron microscopy at low temperatures has been demonstrated to be a useful tool for the study of superconducting materials (Watanabe and Ishikawa, 1967), solidified gases and temperature dependence of the absorption phenomena (Watanabe, 1965). While liquid helium stages have been constructed for other microscopes, no such stage has been reported for the Philips E.M. 300 electron microscope. The first part of this thesis describes a liquid helium stage built for the Philips microscope.

The main problem of designing a low temperature stage for this microscope is that the space available for such a stage is much smaller than the corresponding spaces available in other electron microscopes for which low temperature stages have been designed. In these microscopes the specimen is inserted into the bore of the objective lens via an airlock above the upper polepiece. A large amount of space is available in the region of the air-lock thus it is a relatively easy task to install a liquid helium cooling device. In the Philips microscope the objective lens coil is mounted above the upper pole piece of the objective lens hence for the low temperature stage

described in this thesis, the specimen, the tube for the liquid helium, the radiation shield for the specimen and the objective aperture are all situated between the objective lens pole pieces which have a separation of only 7 mm. For the purposes of comparison with the present stage some helium stages designed for other microscopes will now be described.

The first liquid helium stages developed sacrificed some of the conveniences of room temperature stages in the process of obtaining low temperatures. Thus the stages designed by Piercy et al., (1963), Cotterill (1964), Valdrè and Goringe (1965) and Boersch et al., (1966/67) did without the specimen exchange mechanism, and only the stage of Valdrè and Goringe (1965) tilted about two axes. Venables' (1963) stage, retained the specimen exchange mechanism and one tilt axis, but the specimen drift was quite severe.

Piercy's apparatus involved the modification of a Siemens' cold finger, to allow liquid helium to flow to the end of the cold finger. Thermal contact between the specimen holder and cold finger was maintained by soldering the two together in situ. However, this method of securing thermal contact ruled out the possibility of tilting. Experiments involving condensed gases indicated that specimen temperatures of about 20°K could be obtained with a helium consumption of 10 litres per hour, which is a relatively high rate. Valdrè and Goringe (1965) retained the tilting mechanisms ($\pm$ 7°) and connected

a liquid helium transfer line to a hollowed-out specimen holder. By regulating the helium flow and by the addition of a small heater they were able to obtain a temperature range of 5 to 300°K. Helium consumption was approximately 5 litres per hour when the specimen temperature was maintained at 5°K. Cotterill also employed the technique of circulating liquid helium within the specimen holder itself but instead of using a transfer tube the liquid helium was stored in a dewar system located just outside the microscope column and connected to the microscope vacuum system.

The first stage designed by Venables (1963) used a liquid helium storage cryostat and retained the exchange mechanism, so that specimens could be changed without having to warm the cryostat and break the vacuum of the microscope. In this case the specimen holder was dropped from the exchange mechanism into a conical holder, cooled by the flow of liquid helium in a small tube coiled around the stage. The flexibility of the tubing allowed translation and tilting about one axis ($\pm$ 10°). Temperatures down to 15°K were obtained with no specimen contamination.

Micrographs have been taken at 4.2°K with 50 Å resolution using a highly stable stage designed by Boersch et al., (1966/67) in which liquid helium is actually stored in a container around the specimen, the exhaust helium gas being used to cool a radiation shield. This stage does not include a tilting mechanism; however, a more elaborate version of this type of stage by

Kitamura et al., (1966) does allow tilting via a gimbal system and a resolution of 30 Å down to 4.2°K is claimed. Watanabe and Ishikawa (1967) have produced a stage which retains the specimen exchange mechanism in which liquid helium circulates in flexible tubing coiled around the specimen holder, as in Venables' first design. Temperatures down to 4.2°K are possible. A later stage by Venables et al., (1968) retains the specimen exchange mechanism, has two axes of tilt (± 8°), and is a highly stable stage which will operate at temperatures between 4.2°K and 50°C. A resolution of 25 Å is claimed for work on solidified gases. Valdrè and Goringe (1970) also have produced an improved stage with similar performance to that of the previous version but which includes the possibility of changing specimens through a small airlock without breaking the microscope vacuum.

The best helium stages described above are versatile, retaining such features as specimen tilt about two axes, specimen exchange via an airlock and have resolving powers of about 25 Å at specimen temperatures as low as 4.2°K. The stage designed in the present work has a resolution of about 60 Å at specimen temperatures of 9°K and does not include a specimen tilting or exchange mechanism. Hence, this stage does not match the versatility or performance of the above mentioned stages but shows that it is possible to build a liquid helium stage for the Philips E.M. 300 electron microscope despite the very small amount of space available in the specimen area.

CHAPTER II

CONSTRUCTION OF THE STAGE

There are two types of liquid helium stages; one includes a small helium storage vessel either inside the microscope (Boersch et al., 1966/67) or outside the microscope (Venables, 1963) to which the specimen holder is attached, and another is the transfer type in which helium is transferred continuously from a large dewars vessel to cool the specimen. The helium storage type using a 700cc cryostat located just outside the microscope column was adopted for this work since it has several advantages over the transfer type.

The storage type is more convenient to use since the large dewars vessel containing the liquid helium and the transfer tubing which takes up a considerable amount of space can be removed from the vicinity of the electron microscope before electron microscope observations are begun. Furthermore, the transfer tube used for the transfer type stage introduces a large moment arm to the microscope which can be the source of troublesome vibrations. Another advantage of using a helium storage vessel is the very low helium consumption of this type of stage. The direct transfer stages designed by Piercy et al., (1963) and by Valdrè and Goringe (1965) use 10 litres per hour and 4-5 litres per hour respectively, while the stage of Boersch

et al., (1966/67) which uses a liquid helium storage vessel located inside the microscope consumes only 1.5 litres per hour. The lowest helium consumption seems to be that for the stage built by Venables et al., (1968) which includes an 800cc liquid helium cryostat situated just in front of the microscope supported on a bracket attached to the lower part of the microscope column. Runs of up to 10 hours at liquid helium temperatures with one filling of the cryostat are possible.

A liquid helium storage vessel surrounding the specimen inside the microscope is ruled out for the Philips machine because of the small amount of space available. The low temperature stage and liquid helium cryostat produced in the present work will now be described.

The specimen stage consists of the older type Philips tilt stage, part number PW 6501, with a modified specimen support and a hole drilled horizontally through one side to bring in the helium tubes and associated shielding from the cryostat. The cryostat, the lower section of which is shown in figure 1, is made of stainless steel and sits on a stand beside the microscope column (see figure 2). It consists of an outer vessel A, in which are located concentrically the vessels B and C containing liquid nitrogen and helium respectively.

Liquid helium flows through the $\frac{1}{16}$ th-inch-diameter cupronickel tube D to a copper end plug E, an enlarged top sectional view of which is shown in the upper part of figure 1, and back

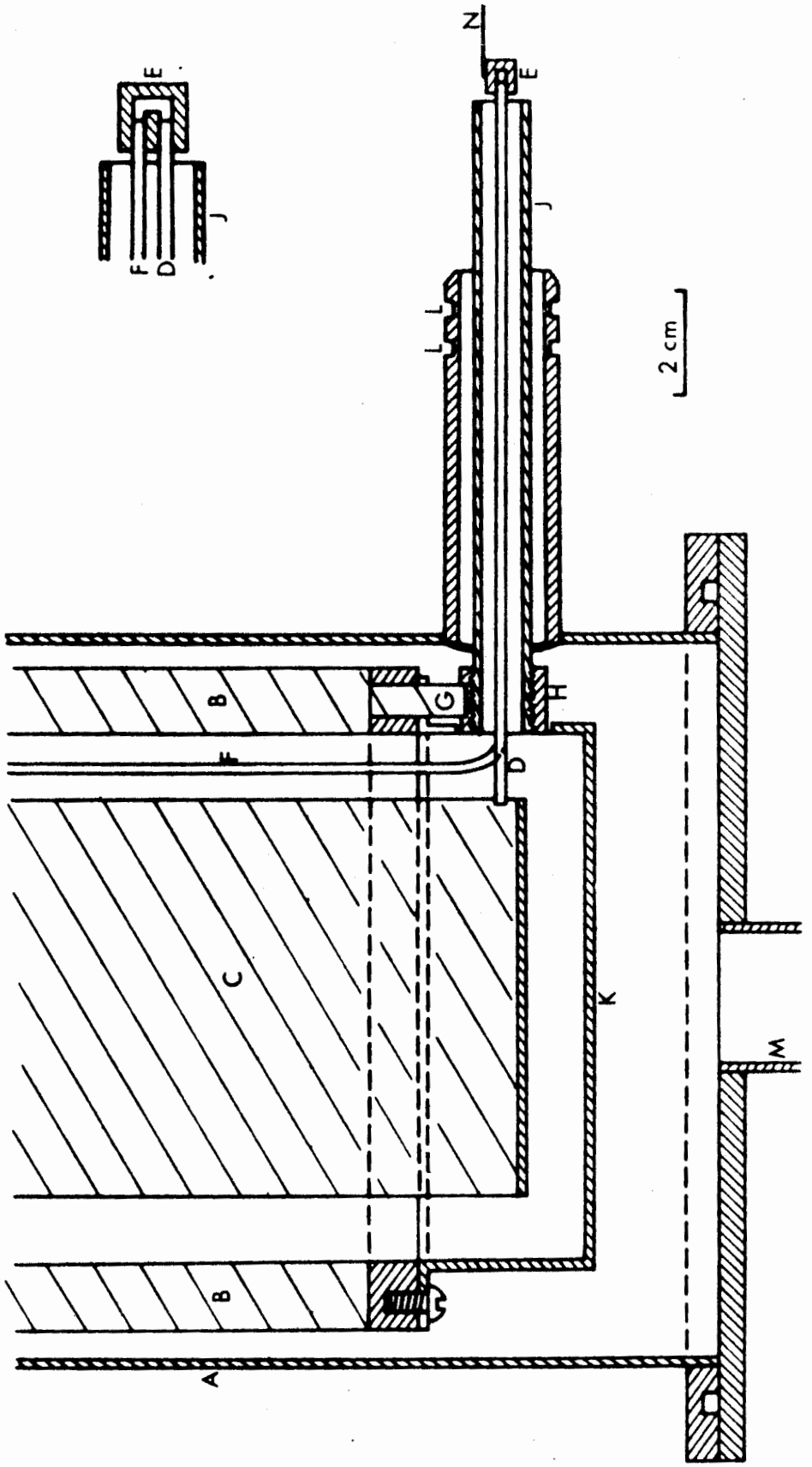

FIGURE 1: Section of the lower part of the liquid helium cryostat.

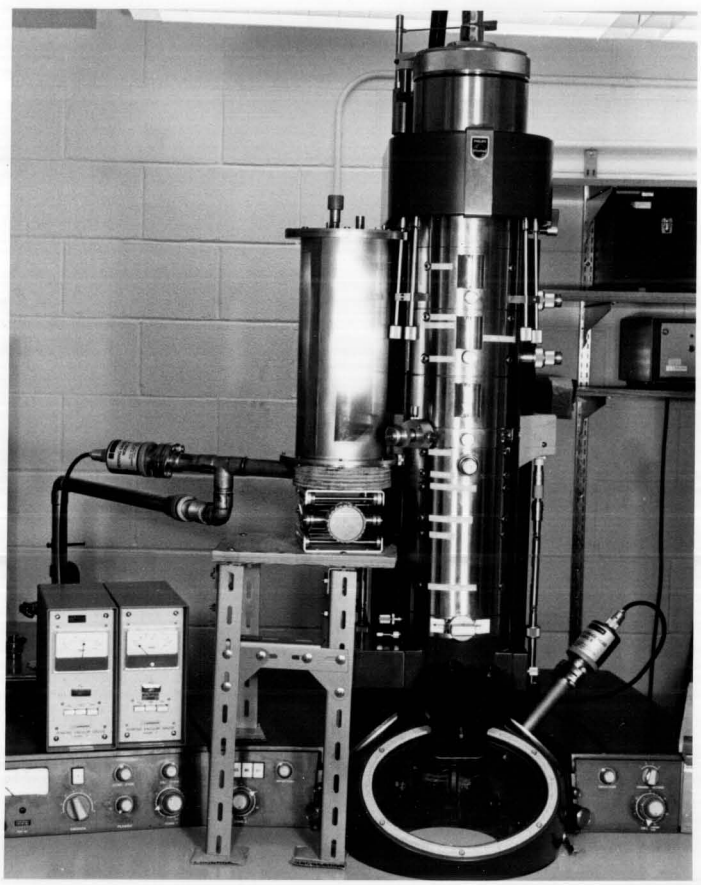

FIGURE 2: Liquid helium cryostat in its operating position beside the electron microscope column.

through an identical tube F to an outlet.

The bottom of the nitrogen vessel B has protruding from it a tube G, which is soldered into the copper collar H. A well annealed $\frac{3}{8}$ th-inch-diameter copper tube J is threaded into H, a grease (Wakefield Thermal Compound No. 122) being used to provide a good thermal contact. An aluminum cap K with a slot cut out to fit over the collar is attached to the bottom of the nitrogen vessel by means of screws. The "0" rings which fit in the grooves L seal against the sides of a hole drilled in the stage. Thus the cryostat is connected to the vacuum system of the electron microscope. The one-inch-diameter pumping line M is connected to an oil diffusion pump which decreases the pump-down time and improves the vacuum in the vicinity of the specimen.

The copper wires N shown in figures 1 and 3 are soldered to the copper end plug E and to the specimen holder Q (see figure 3); they thus conduct heat away from the specimen into E. This method of securing the specimen holder to the helium cooling tubes decreases the vibration transmitted to the specimen from boiling helium and permits specimen translation. The copper pieces P, shown in figure 3 are soldered to the tube J which is at about 77°K; thus, these pieces act as shields against room temperature radiation.

The specimen holder itself consists of a thin copper sheet Q clamped around a piece of mica R, 0.1mm thick, which

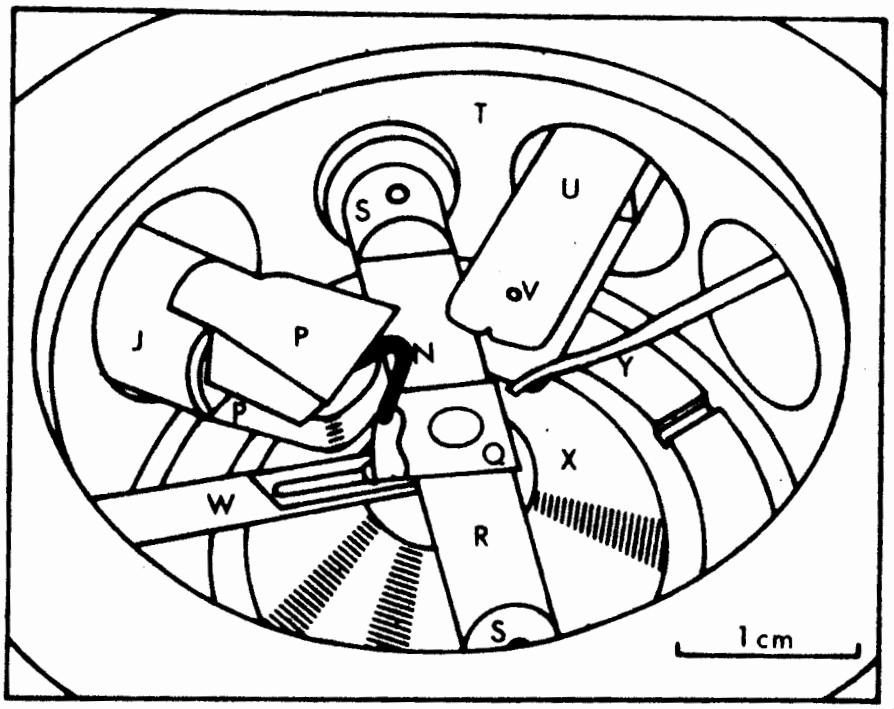

FIGURE 3: View of the specimen chamber with the microscope column split at the objective lens level.

is fastened onto the celeron posts S by means of brass screws (see figure 3). These posts are glued into the object positioning ring T located inside the stage. Specimen movement is accomplished in the usual way by moving the object position ring with the aid of two push-rods against a spring action; smooth movement is ensured by agate stones. A hole, approximately 3mm in diameter passes through both Q and R and a copper specimen grid which carries a thin carbon film is mounted across this hole by means of Wood's metal which solders the grid to the copper sheet Q. Electrostatic charging due to the accumulation on electrical insulators of electrons from the electron beam is prevented by a coating of silver previously applied to the mica R and the celeron posts S by means of vacuum deposition. The specimen is shielded from room temperature radiation and from contamination by the Philips cooling blades U which are shown in the withdrawn position in figure 3. When the blades are advanced (see figures 4 and 5) the electron beam passes through the hole V in the upper blade and after travelling through the specimen exits through a second hole in the lower blade. The objective aperture holder W is positioned between the objective lens lower polepiece X and the lower blade of the cooling blades U (figure 3). A small gas inlet tube Y enters the microscope through a pumping hole which is connected to the diffusion pump of the electron microscope. Preliminary tests carried out which will now be described

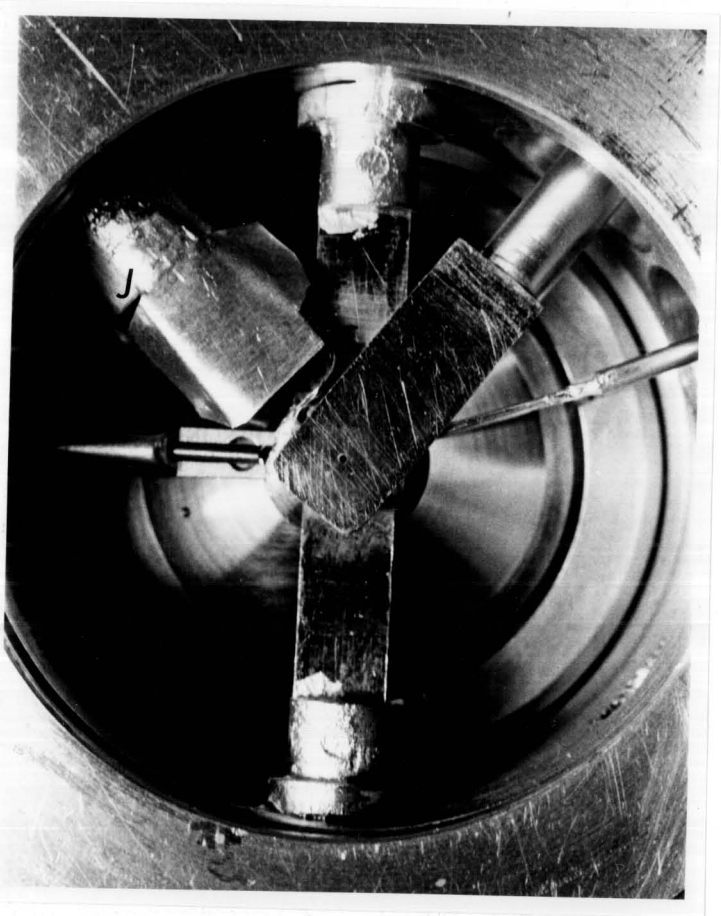

FIGURE 4: The specimen chamber with the cooling blades advanced. The copper tube J surrounds the helium tubes (see also figure 1 and 3).

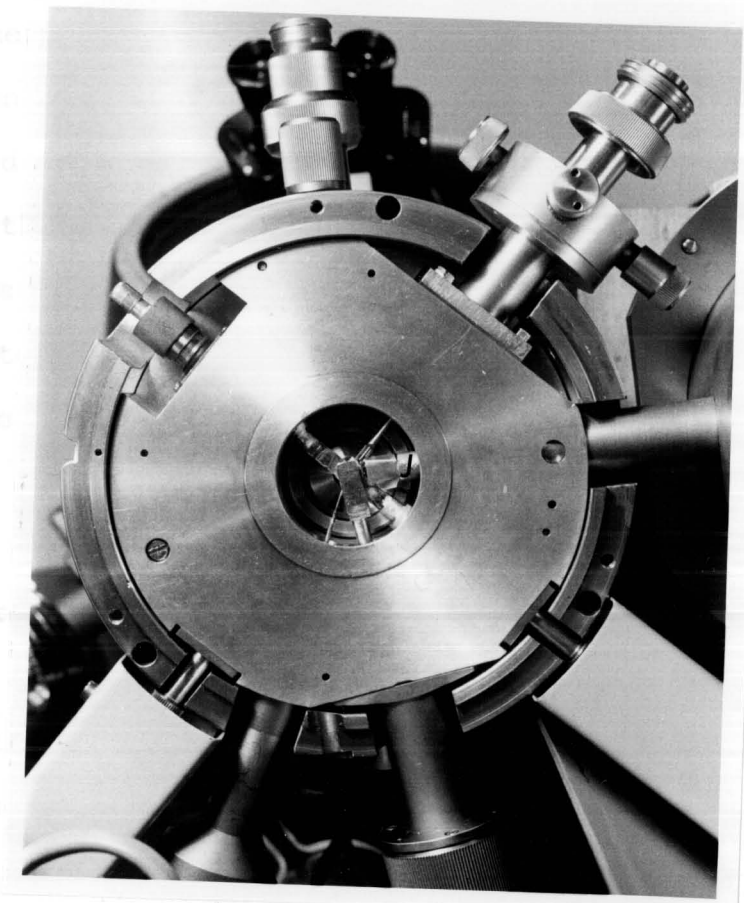

FIGURE 5: Overall view of the low temperature specimen stage in its operating position in the electron microscope.

showed the effectiveness of this gas inlet system.

In order to test the system, the microscope was split at the objective lens level and the top of the specimen stage was sealed by means of a glass blank and an "0" ring so that gas condensation could be observed visually. The stage was cooled using liquid nitrogen instead of helium and the gas introduced into the microscope was carbon dioxide. In the first test the gas inlet tube Y was not installed, the carbon dioxide being admitted into the microscope via a hole drilled in the pumping tube connecting the specimen chamber to the diffusion pump of the electron microscope. The pressure measured at the cryostat by a Penning gauge connected to the pumping line M decreased from $\sim 10^{-5}$ torr to $\sim 10^{-4}$ torr while the carbon dioxide was allowed to enter the microscope. After several minutes at this pressure a heavy white deposit could be observed on the edges of all the liquid nitrogen cooled surfaces including the edge of the copper sheet Q facing the pumping hole. However, because of the shielding effect no observable deposit formed on the top surface of Q or on the carbon coated copper grid soldered to Q. The fact that no carbon dioxide was condensing on the specimen was verified by electron diffraction observations carried out with the microscope in full operation. The gas inlet tube Y directing the gas onto the specimen was then fastened to the gas inlet hole in the pumping tube by means of Torr Seal and similar tests were again carried out.

In this case a carbon dioxide deposit could be observed on the specimen a few seconds after turning on the gas flow and with a rate of flow, as judged by the opening of the needle valve, much smaller than for the case with the tube Y removed. Figure 6 is a micrograph of solid carbon dioxide and figure 7 is the corresponding diffraction pattern taken at liquid nitrogen temperature.

After the microscope column had been baked out for about five hours, a pressure of less than 10^{-6} torr could be obtained in the microscope, the shielding being cooled to liquid nitrogen temperatures. Baking out the column is a standard procedure for the Philips microscope achieved by turning on the lens currents after short circuiting the water supply used to cool the lenses. This baking out procedure improved the vacuum and also decreased considerably the contamination rate on the specimen due to water vapour, this rate being very high immediately after the microscope had been up to atmospheric pressure.

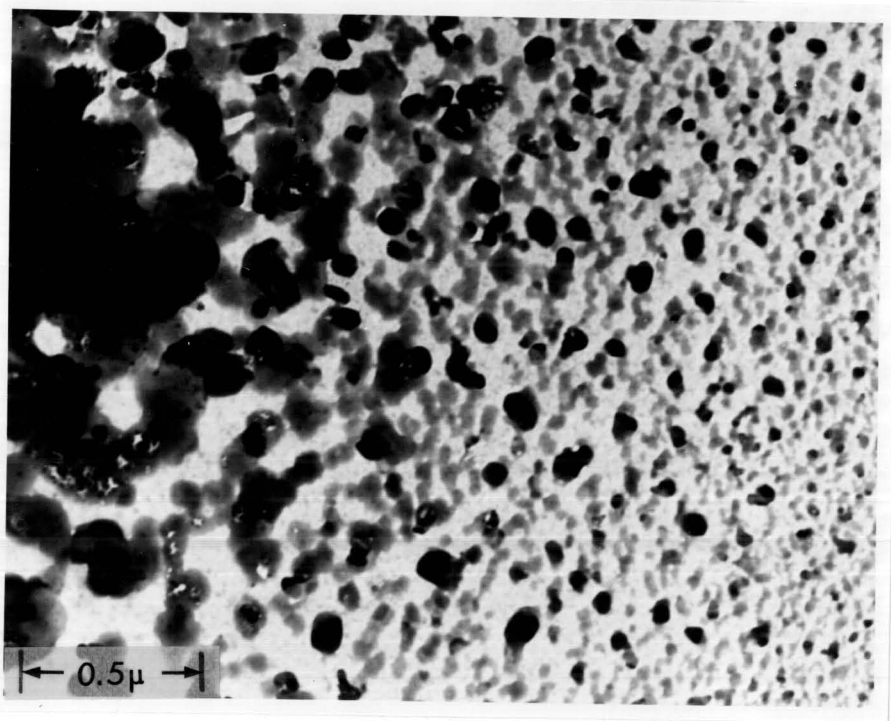

FIGURE 6: Micrograph of solid carbon dioxide taken at liquid nitrogen temperature. Magnification = × 47,000.

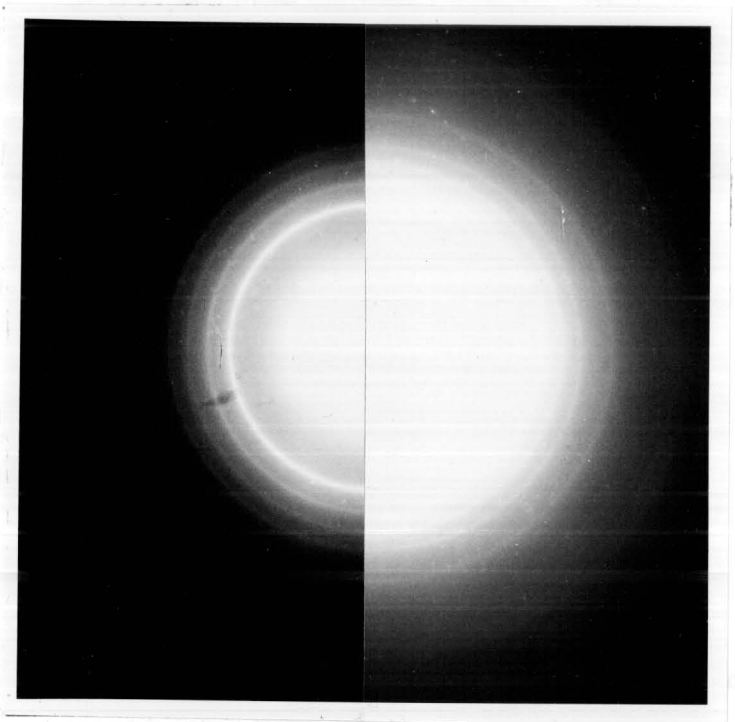

FIGURE 7: Diffraction pattern from solid carbon dioxide at liquid nitrogen temperature.

CHAPTER III

OPERATION OF THE STAGE

III-1 Cooling Procedure

Liquid nitrogen is poured into the reservoir B to cool the various radiation shields. Liquid nitrogen is also used to lower the temperature of the blades U. During this precooling, residual gases condense on the shielding and the contamination on the specimen is thus reduced. Liquid helium is transferred into the reservoir C after precooling it with liquid nitrogen. The helium cooled surfaces tend to reduce the pressure still further so that the final pressure in the specimen chamber is less than 10^{-6} torr.

The specimen is cooled by closing off the top of the liquid helium reservoir C. When this is done the pressure over the liquid builds up and consequently the liquid is forced through the tube D round the cap E and then through the exit tube F (see figure 1). When the top of the liquid helium reservoir is again opened and when the outlet tube F is closed the helium flow through E ceases and consequently the temperature of the specimen increases. Condensed gases such as nitrogen are removed from the specimen within one minute after the supply of liquid helium to E is cut off.

III-2 Performance

The magnification of the stage was calibrated at room temperature for the Selected Area range switch settings by first noting the width of a square of a copper specimen grid at the lowest magnification and comparing this measurement to the average width of a square measured with the aid of a travelling microscope. As the size of the image was increased the magnification was found by measuring distances on the plate between certain identifiable areas on the specimen. This produces a rough calibration of about 10% accuracy. Figure 8 shows the results as a plot of the magnification against the selected area setting for the helium stage.

In order to measure the sample temperature, the gases carbon dioxide, krypton, argon, nitrogen and neon were introduced into the microscope through the tube Y via an Edwards fine control needle valve located outside the microscope. The gases were of industrial grade and were obtained from Matheson Gas Products, Whitby, Ontario. Observation of the diffraction pattern during condensation enabled the gas flow to be cut off before the condensate layer became opaque to the beam.

The gases carbon dioxide, krypton, argon and nitrogen could be observed for an indefinite length of time at normal beam currents but could be removed by the heating effect of an intense electron beam. Figure 9 shows micrographs of solid carbon dioxide before and after removal with an intense electron beam.

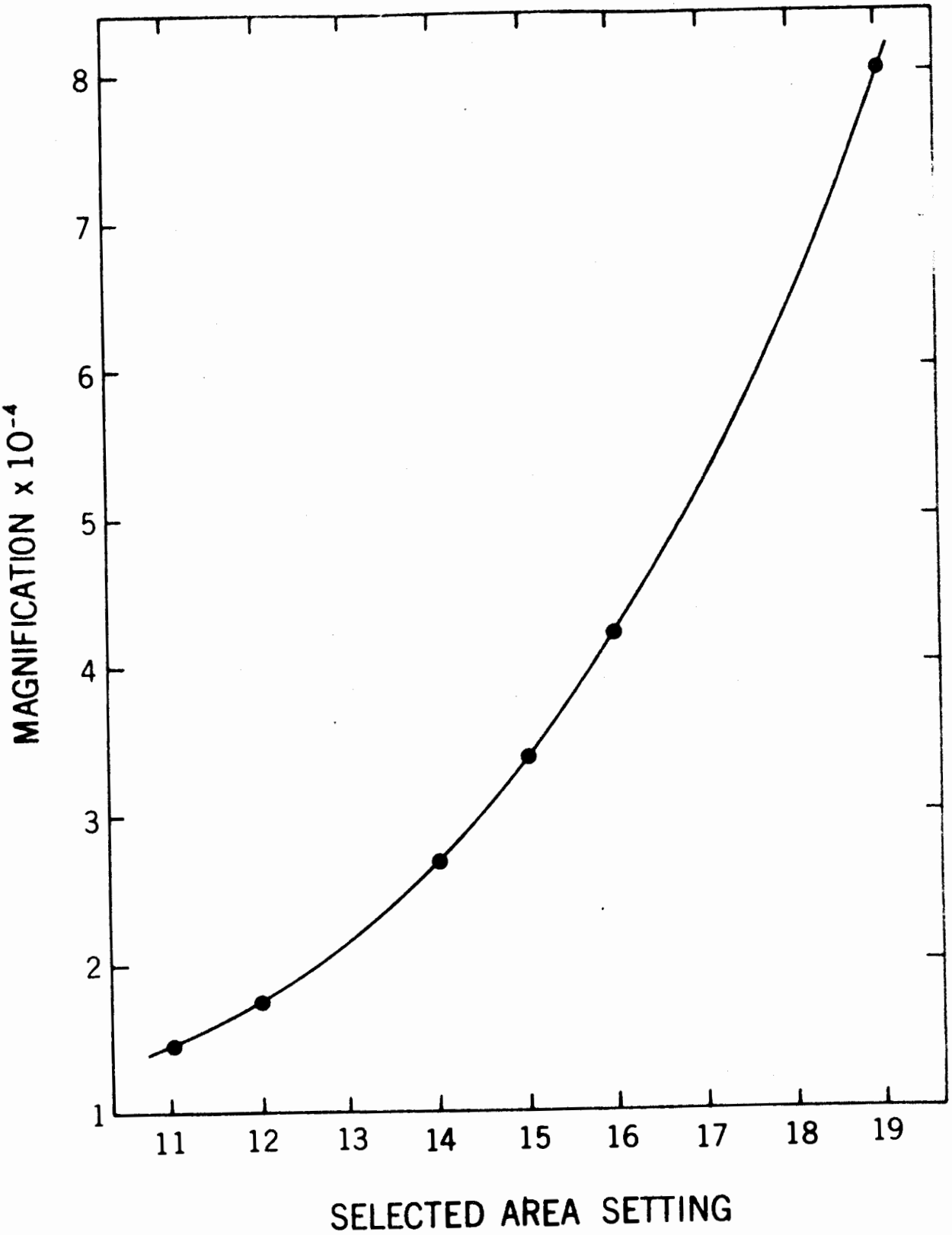

FIGURE 8: Magnification Calibration of the liquid helium stage for the Philips E.M. 300 electron microscope.

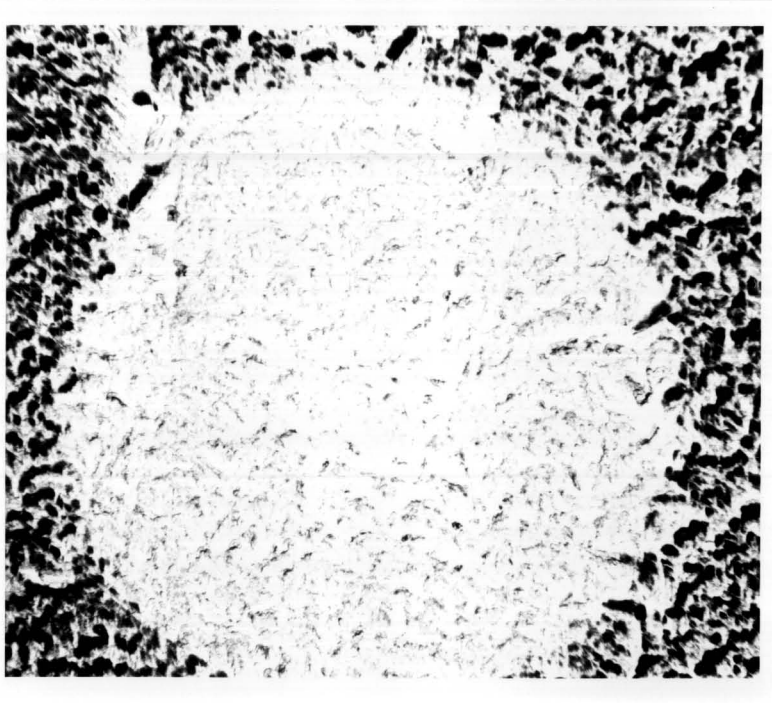

FIGURE 9: Solid CO_2 before (a) and after (b) removal with an intense electron beam.
Magnification = × 1380.

Neon could be observed only for a few seconds even with a low beam intensity, however, it remained indefinitely on areas not illuminated by the beam. This shows that areas of the specimen not illuminated by the beam were at least as low as 9°K, the sublimation temperature of neon at 10^{-5} torr (Honig and Hook, 1960). Just how low a temperature can be obtained is limited primarily by the heat input to the specimen from the electron beam. In principle the temperature rise due to beam heating could have been decreased by using as a substrate a thick metal foil with small thin regions instead of the carbon film used in the present experiment. This type of substrate is made by putting small indentations in 0.005-inch-thick foils of pure metals, which are then annealed and finally electropolished. This produces a small hole at the indentation, surrounded by a narrow region of thin foil with comparatively thick (0.003-inch) foil elsewhere (Venables, 1963).

The crystal structures of the observed gases have been studied in detail by others (see for example Curzon and Pawlowicz, 1965; Curzon, 1969; etc.) The crystal structure of carbon dioxide (Curzon, 1970) and of α nitrogen (stable below 35.5°K) is cubic with space group T_h^6. The centres of the nitrogen molecules lie on a face-centred-cubic lattice but the axes of the four molecules per unit cell point in different <111> directions. Figure 10 is a diffraction pattern from α nitrogen obtained in the present experiment and figure 11 is the

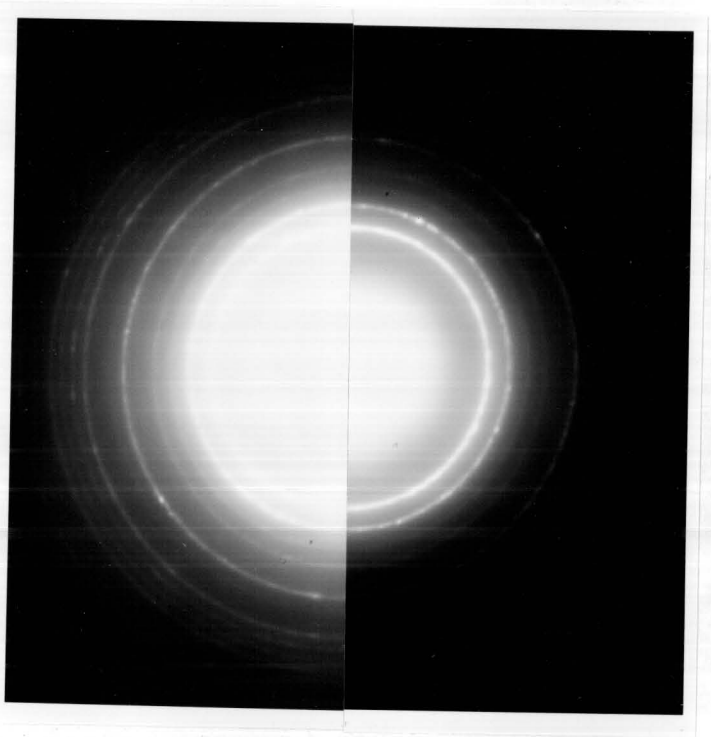

FIGURE 10: Diffraction pattern from α-nitrogen.

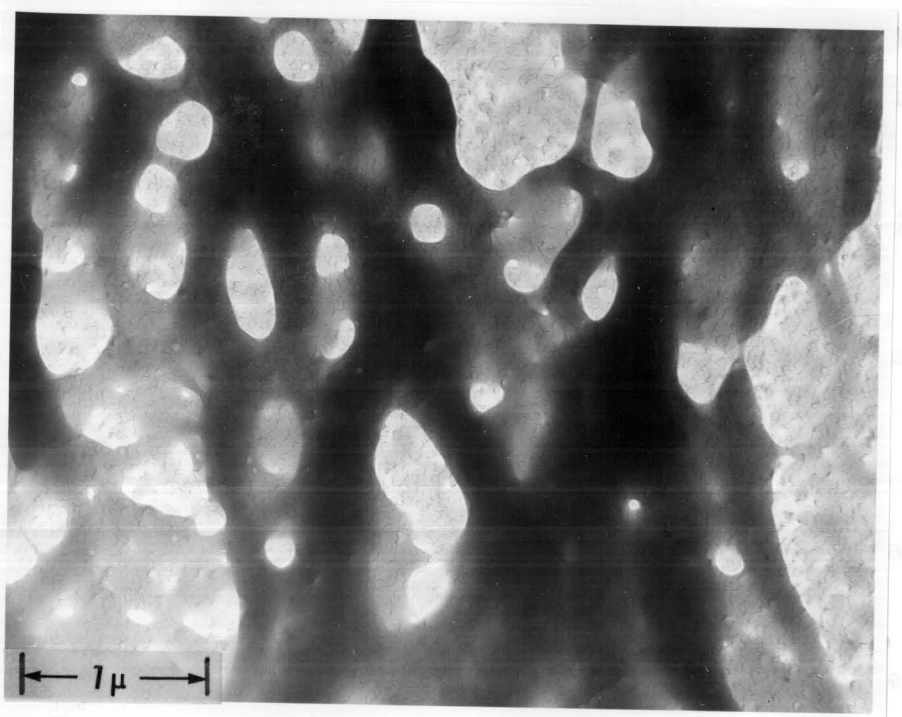

FIGURE 11: Micrograph of α-nitrogen deposit showing voids due to sublimation. Magnification = × 24,400.

corresponding migrograph. Electron diffraction patterns from deposits of argon, krypton and neon in the condensed state were found to be consistent with a face-centred-cubic lattice. Figures 12 and 14 are diffraction patterns and figures 13 and 15 are micrographs of solid argon and krypton respectively. Figure 16 is a diffraction pattern from solid neon; a micrograph of neon was not obtained because the solid sublimed too quickly to allow the long exposure necessary at low beam intensity.

The resolution of the stage is about 60 Å as can be seen on the enlarged micrograph of krypton shown in figure 17. The print of the micrograph has a final magnification of 112,000 and was taken with a two second exposure, the Selected Area range switch being set at 14.

The nitrogen shielding surrounding the specimen keeps contamination at a low level, making it possible to make runs of up to one hour without any noticeable contamination forming on the specimen. Helium consumption is relatively low compared to that for other low temperature stages; in one experimental run lasting two and one-half hours, three and one-half litres of liquid helium were used to fill the 700cc helium reservoir.

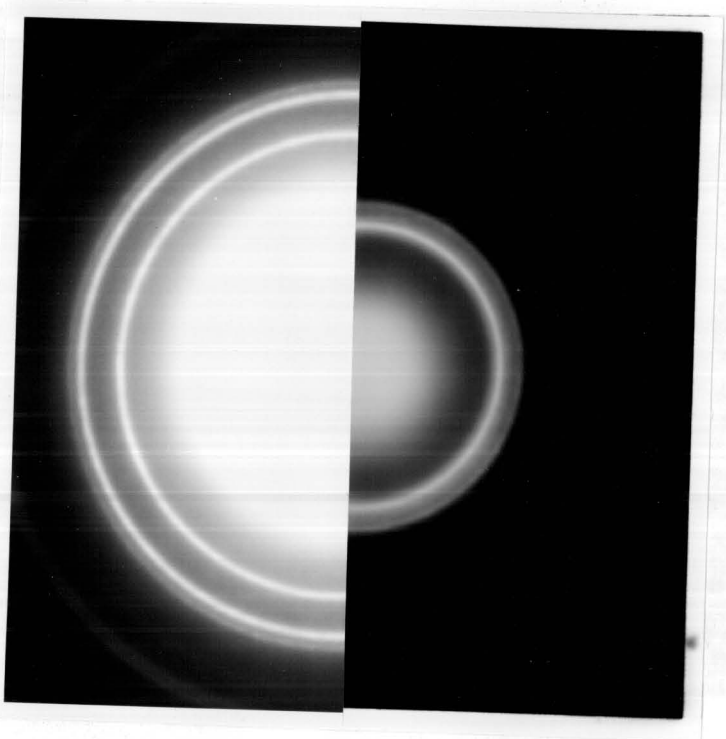

FIGURE 12: Diffraction pattern from solid argon.

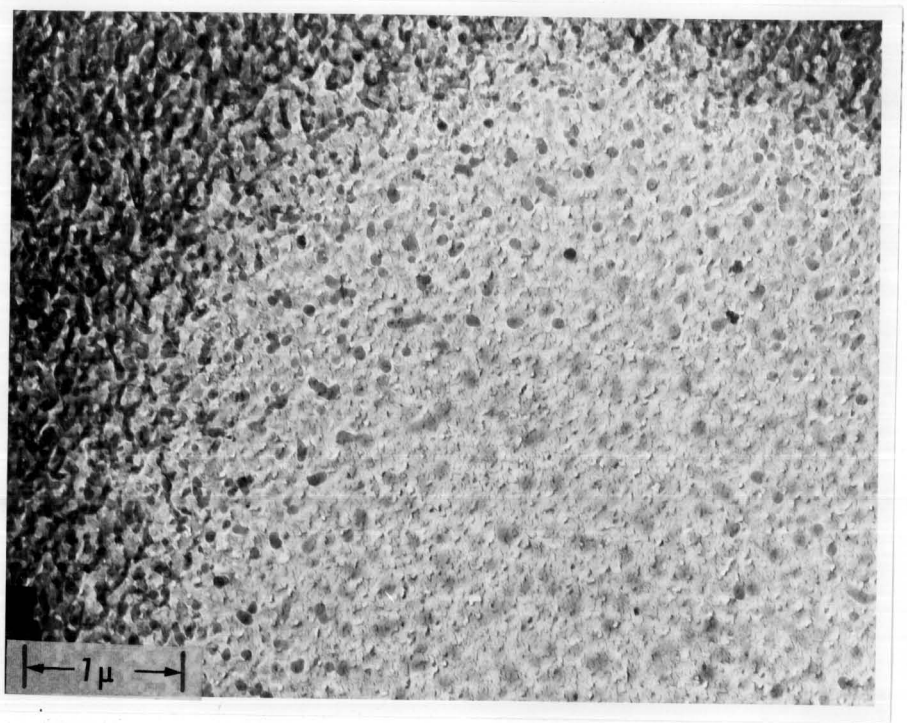

FIGURE 13: Micrograph of solid argon partially removed due to the heating effect of the electron beam.
Magnification = × 20,400.

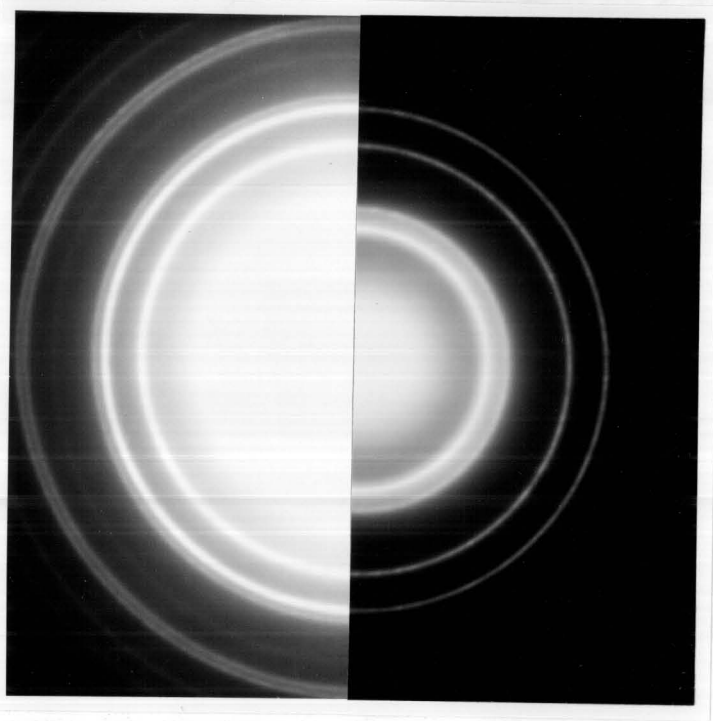

FIGURE 14: Diffraction pattern from solid krypton.

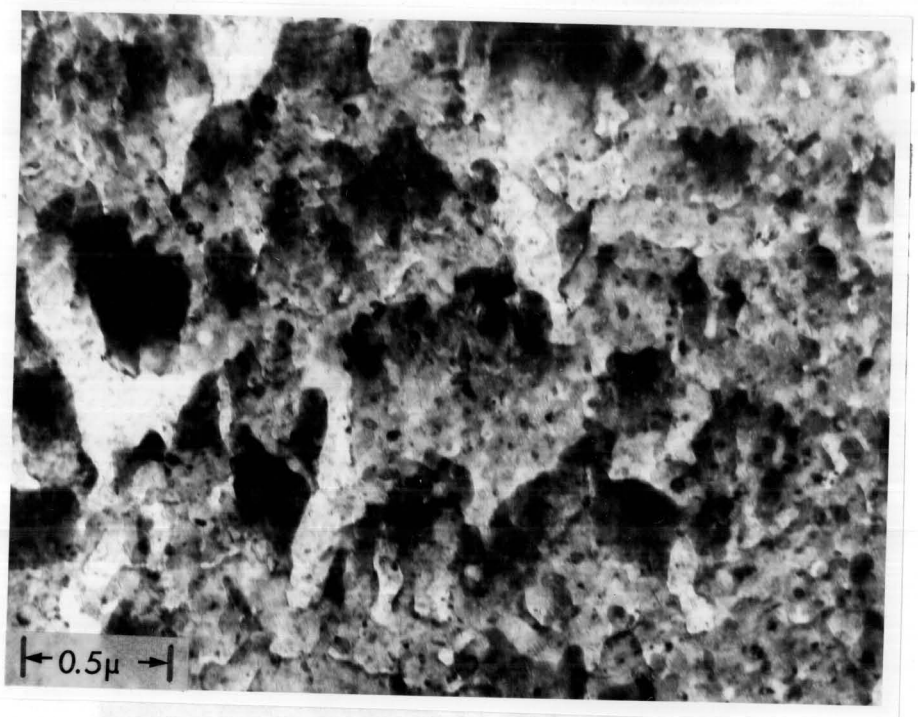

FIGURE 15: Micrograph of solid krypton.
Magnification = × 37,400.

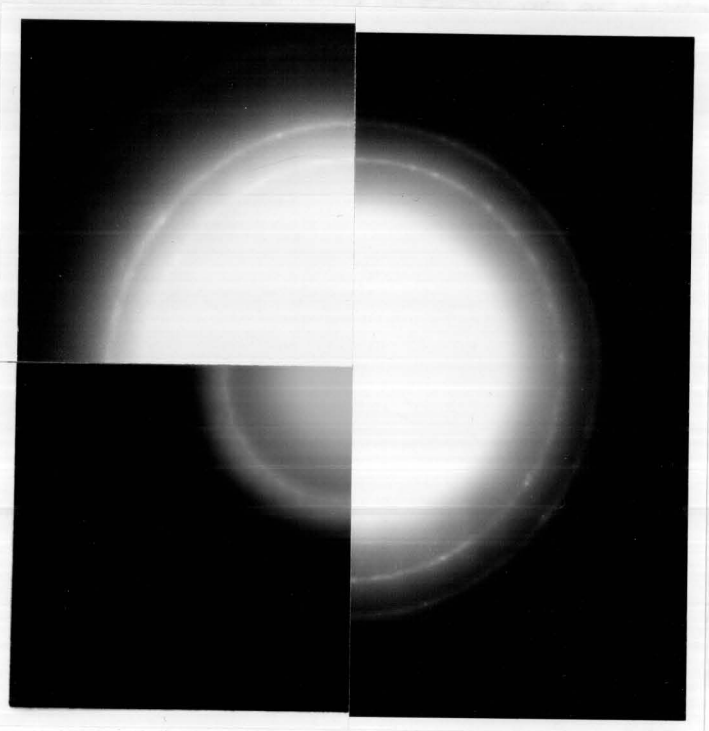

FIGURE 16: Diffraction pattern from solid neon.

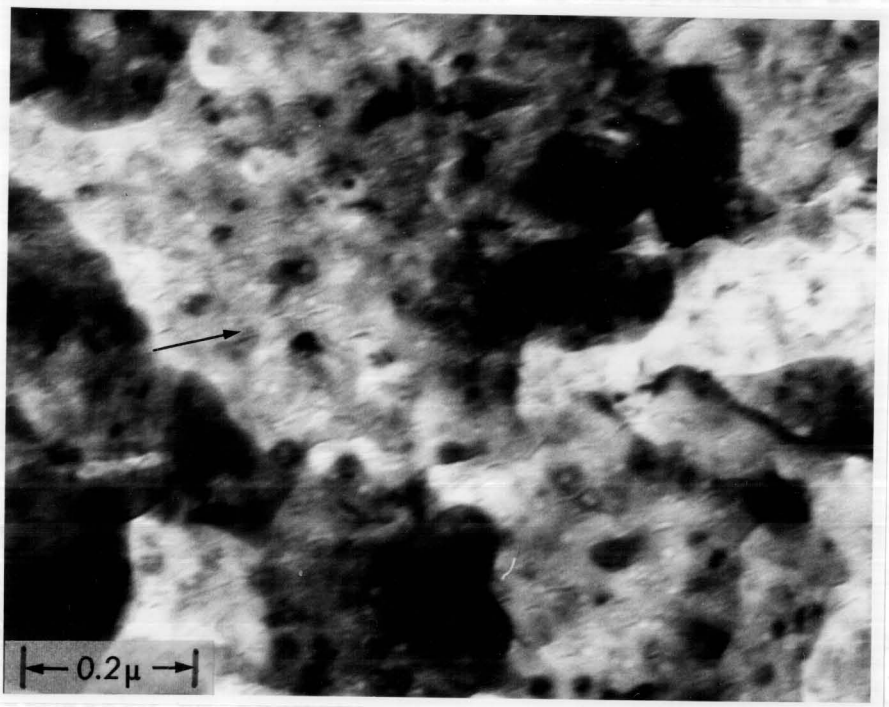

FIGURE 17: Enlarged micrograph of krypton. The arrow indicates two particles separated by 60 Å. Magnification = × 112,000.

CHAPTER IV

CONCLUDING REMARKS

The present work has shown that it is possible to build a liquid helium stage for the Philips E.M. 300 electron microscope despite the very small amount of space available in the specimen area. The present low temperature stage has a reasonably good resolution of 60 Å and fair stability at a specimen temperature at least as low as 29°K, the sublimation temperature of nitrogen at 10^{-5} torr. Observations down to 9°K are possible although at present it is not possible to obtain micrographs at this temperature. However, micrographs at such low temperatures would be a distinct possibility with the use of metal foil substrates rather than the carbon film used in this experiment. Helium consumption is relatively low at 1.4 litres per hour.

Although the stage has certain disadvantages, including no facility for specimen tilting and lack of a specimen exchange mechanism via an airlock these and other features are a distinct possibility for future improvements of the stage now that a working prototype has been constructed. The thin mica strip supporting the specimen holder could be replaced by a glass rod mounted in such a way that specimen tilt about a single axis is possible and the rigidity of such a rod would decrease vibration hence increasing the stability and resolution of the

stage. A hole for such a rod to pass through already exists in the stage since the specimen is inserted by means of a metal rod in the original room temperature stage. A specimen exchange mechanism presents a more difficult problem due to the small space available but should also be a possibility. The addition of a small heater to increase the temperature range of the specimen and a thermocouple to measure the temperature and perhaps even an evaporator should present no great problems to the designer.

PART B. A STUDY OF FACE-CENTRED-CUBIC THIN FILMS OF SOME RARE-EARTH METALS AND THEIR OXIDES

CHAPTER I

INTRODUCTION

Materials in the form of thin films sometimes occur with crystal structures which differ from those of the normal bulk structures. The present investigation was carried out in order to determine whether the metals gadolinium, terbium, dysprosium, holmium, erbium and thulium, which in bulk form have a hexagonal structure, would have the closely related face-centred-cubic structure in thin films.

Spheres may be close-packed to form either a hexagonal-close-packed lattice or a face-centred-cubic lattice, the relations between the lattice parameters being $a_o = \sqrt{2}\ a$ and $c = \sqrt{8}\ a/\sqrt{3}$ where a_o is the lattice parameter of the cubic lattice and a and c are the lattice parameters of the hexagonal lattice. It is also true that $a_o = \sqrt{2}\ d_n$ where d_n is the nearest-neighbour distance in either of the lattices.

The crystal structure of the metals under investigation in bulk is hexagonal with the metal atoms at 000 and $\frac{1}{3}\ \frac{2}{3}\ \frac{1}{2}$ and lattice parameters listed in table 1 (Spedding and Beaudry, 1971). The ratios c/a for the metals given in table 1 lie in the range 1.569 to 1.591. This does not correspond to the close packing of spheres for which c/a is 1.633, hence it is

TABLE 1: Lattice parameters in Å of the metals Gd, Tb, Dy, Ho, Er and Tm in bulk form (Spedding and Beaudry, 1971). The lattice parameters a_o of the f.c.c. form of these metals is expected to be in the neighborhood of $\sqrt{2}$ a and $\sqrt{2}\, d_n$ where d_n is the nearest neighbour distance in the hexagonal form.

Metal	a	c	c/a	$\sqrt{2}$a	$\sqrt{2}\, d_n$
Gd	3.634	5.781	1.591	5.14	5.05
Tb	3.606	5.697	1.580	5.10	4.99
Dy	3.592	5.650	1.573	5.08	4.96
Ho	3.578	5.618	1.570	5.06	4.93
Er	3.559	5.585	1.569	5.03	4.90
Tm	3.538	5.554	1.570	5.00	4.88

not possible to use the lattice parameters of the hexagonal form to obtain accurately the lattice parameter a_o of a possible f.c.c. form of any of these metals. However, the relations $a_o = \sqrt{2}\, d_n$ and $a_o = \sqrt{2}\, a$ which were discussed above and which apply strictly to spheres should at least give first order approximations to a_o where d_n is the nearest neighbour distance in the hexagonal form of the metal. The result obtained is that a_o is expected to be in the neighbourhood of the values shown in table 1. The experimental values of a_o for the metals Tb, Dy, Ho, Er and Tm are in fact $\sim$2% higher and that for Gd $\sim$ 5% higher than the calculated values.

CHAPTER II

EXPERIMENTAL PROCEDURE

The rare-earth films studied in the present experiments were prepared in a vacuum coating unit which operated at 2×10^{-6} to 5×10^{-6} torr. The metals were of industrial grade and were supplied by the American Potash and Chemical Corporation. They were evaporated from a molybdenum filament and the vapour was condensed on thin carbon films supported by electron microscope grids. A shutter between the vapour source and substrate enabled condensation to be started and stopped at any convenient time. With the exception of gadolinium the metals under consideration acted as getters, hence when evaporation started the pressure in the vacuum system generally fell by about a factor of ten. This being the case the metal vapour was in most cases not allowed to condense on the substrate until the pressure had first dropped. When a thin film was condensed in a poor vacuum ($\sim 10^{-3}$ torr) from the moment the metal began to evaporate from the filament, extra diffraction rings belonging to the sesquioxide (for example, Er_2O_3) were observed. Hence, oxygen is the main material absorbed during gettering. This effect is discussed in more detail in Chapter III. A marked gettering action was not observed for gadolinium.

After a metal film was made it was coated with a thin film of vacuum deposited carbon. The final specimen on an electron

microscope grid therefore consisted of a thin film of a rare-earth metal sandwiched between two thin carbon films. When the specimen was removed from the vacuum coating unit and transferred to a Philips E.M. 300 electron microscope the carbon coatings reduced to a minimum the possibility of oxidation by exposure of the specimen to the atmosphere. In preliminary work on erbium a protective coat of carbon was not applied after the metal had been deposited. It was considered that the erbium would rapidly become coated by a thin layer of oxide when the metal was exposed to air and this oxide would prevent oxidation of the entire metal. Electron diffraction studies failed to reveal the presence of oxide in films which were not protected with carbon and hence showed that the above suggested protection mechanism based on a surface oxide film (too thin to be detected) operated reasonably effectively.

The results of an experiment now to be described show that the carbon coating was very effective for reducing oxidation. A layer of carbon was deposited on a glass slide and then two silver electrodes were vapour deposited on the carbon, one at each end of the slide. Copper wires were fastened to the silver electrodes with colloidal silver so that the electrical resistance of the vacuum deposited metal film could be measured during the evaporation. The resistance of the carbon film was too high to be measured. When a thin film of a rare-earth metal was deposited the electrical resistance rapidly

dropped to a measurable level even for very thin films (~50 Å) showing that the rare-earth films became continuous at relatively thin average thicknesses. For example, an erbium film 1.5 cm by 2 cm and 200 Å thick had a resistance of about 200 ohms and hence a resistivity of 5.3×10^{-4} ohm-cm. As soon as air was admitted to the coating unit the electrical resistance of the metal film rapidly increased by one or two orders of magnitude showing that the film was much affected by the air. Since in the preliminary experiments on erbium extensive diffraction patterns from erbium oxide were not observed in the erbium films exposed to air in this way it is deduced that the increase in resistance was associated with changes in electrical continuity caused by surface oxidation of metal crystallites especially at grain boundaries and was not due to total conversion of the relatively good conducting metal to the poorly conducting oxide.

When a layer of carbon was deposited on a film of a rare-earth metal immediately after the metal had condensed on the carbon substrate the response of the specimen to exposure to the atmosphere was quite different. The resistance of the specimen only increased by a factor of two or less when exposed to the air instead of by one or two orders of magnitude as had been the case for unprotected films. Unless otherwise stated the results discussed below were obtained from metal films which were protected on both sides by thin

layers of carbon.

The lattice parameters a_o of the f.c.c. form of the metals were determined from the relation (Hirsch et al., 1965, p. 109),

$$R_{hkl} = \frac{\lambda L}{a_o} (h^2 + k^2 + \ell^2)^{\frac{1}{2}}$$

where R_{hkl} is the radius of a diffraction ring arising from reflections from planes with Miller indices hkl and λL is the diffraction constant of the electron microscope. Thallium chloride was used as a calibration material for measurement of the diffraction constant and was deposited directly on the specimens over the protective carbon films, a part of each film being shielded from the thallium chloride vapour. Such a specimen is particularly useful because diffraction patterns may either be obtained from the rare-earth metal alone or from the metal and thallium chloride together, hence difficulties associated with the determination of which rings belong to the metal in a composite pattern are easily resolved.

CHAPTER III

EXPERIMENTAL RESULTS

Figure 1 shows the kind of electron diffraction pattern obtained from a thin film of erbium. The metals Gd, Tb, Dy, Ho, Er and Tm all formed polycrystalline face-centred-cubic films when the deposits were thin. The lattice parameters a_o of the f.c.c. forms are given in table 2. Also appearing in table 2 are the nearest neighbour distances $a_o/\sqrt{2}$ in the cubic structures and the a spacing of the hexagonal structures (Spedding and Beaudry, 1971). As may be seen from the table $a_o/\sqrt{2}$ is 1-2% larger than a for all the metals studied except for gadolinium where the difference is 5%. The values of a_o were measured to about 1% hence it is thought that the result for gadolinium does not differ from the results for the other metals because of a measuring error but because a real effect exists. The difference is thought to be due to oxygen contamination of gadolinium. When gadolinium is evaporated it does not act as a getter hence the chance of contamination is higher, in fact, in some regions of the gadolinium specimen oxide rings could be observed. It is pointed out in section IV-4 that oxidation of the face-centred-cubic form of erbium leads to a slight rearrangement of the erbium

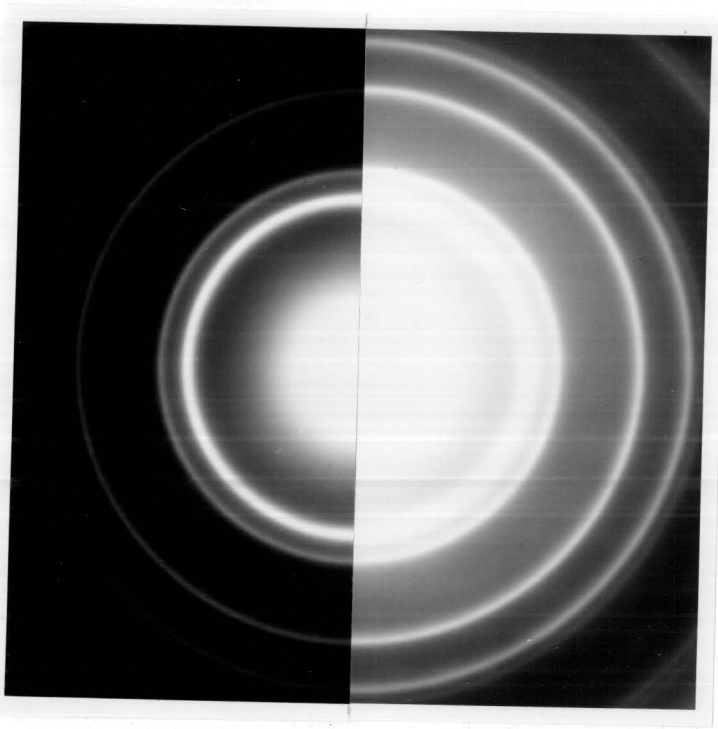

Figure 1: Electron diffraction pattern from a thin film of f.c.c. erbium. 100 kV electrons.

TABLE 2: Lattice parameters in Å for rare-earth metals. a_o is the lattice parameter of face-centred-cubic metals observed in thin films; a is the lattice parameter of hexagonal-close-packed metal observed in bulk (Spedding and Beaudry, 1971).

Metal	a_o	$a_o/\sqrt{2}$	a
Gd	5.40	3.82	3.634
Tb	5.20	3.68	3.606
Dy	5.18	3.66	3.592
Ho	5.15	3.64	3.578
Er	5.09	3.60	3.559
Tm	5.06	3.58	3.538

atoms but basically the erbium lattice remains almost face-centred-cubic with a lattice parameter which is 4% bigger than in the pure metal. A similar state of affairs applies to gadolinium. The observed lattice parameter of 5.40 Å is probably larger than it should be because of oxygen contamination, the oxygen not being present in sufficient quantities to lead to a well defined oxide structure with prominent oxide diffraction rings.

Further support for the suggestion that the observed lattice parameter of face-centred-cubic gadolinium may be slightly larger because of oxygen contamination is afforded by the fact that the lattice parameters of the face-centred-cubic forms of all the other metals listed in table 2 increase by about 2% if these metals are deposited in poor vacuum, that is a vacuum where the gettering effect has not reached maximum efficiency.

When thicker films of rare-earth metal were deposited, both f.c.c. and h.c.p. metal were observed together. This is illustrated by the diffraction pattern of erbium shown in figure 2. The rings from the cubic form are sharper than those from the hexagonal form indicating that the cubic crystals were larger, also the rings from the cubic phase are slightly arced which indicates a tendency towards preferential orientation. The thickest films studied possessed the normal h.c.p. structure.

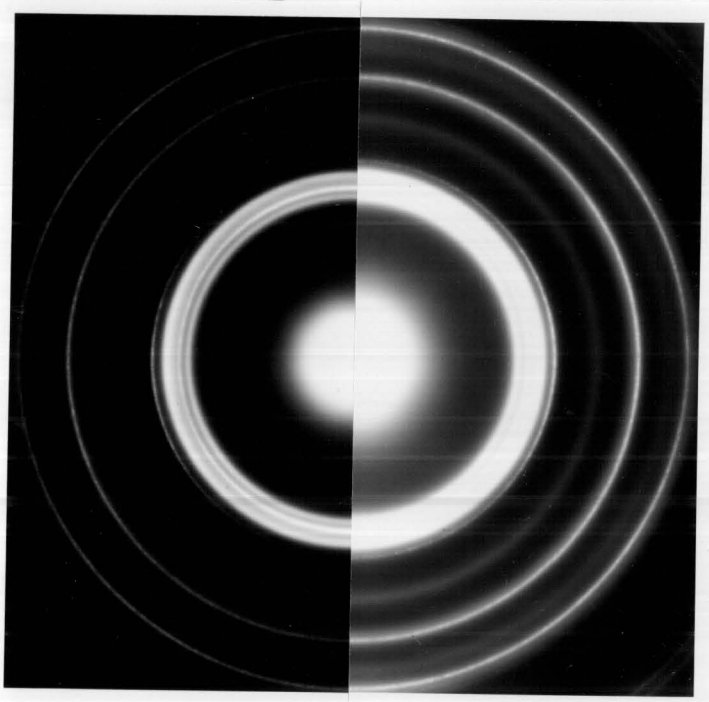

Figure 2: Electron diffraction pattern showing f.c.c. and h.c.p. erbium. 100 k.V. electrons.

All the results described above were obtained when the rare-earth metals were condensed in good vacuum conditions and when the 100 kV electron beam was kept to a low intensity during examination of the films. Figure 3 shows the kind of diffraction pattern observed when a weak electron beam was used to examine a thin film of erbium which had been condensed from the moment erbium began to evaporate from the molybdenum filament. In this case the gettering effect of the erbium did not have sufficient time to come to maximum efficiency, hence the pattern shows evidence of contamination. The brightest ring of the pattern is the 111 ring from f.c.c. erbium. The brightest ring due to contamination is situated inside this 111 ring and is in fact the 211 ring from cubic erbium oxide (Er_2O_3). This same type of contamination was observed for the other metals under consideration when condensation was started the moment the metal began to evaporate.

In all the above results it has been pointed out that the diffraction patterns were obtained by means of a weak electron beam. The reason for this precaution was that the use of a strong electron beam led to the oxidation of the rare-earth metal films because of the heating effect of the beam. Figure 4 shows the diffraction pattern of a film of erbium oxide produced by an intense electron beam acting on a face-centred-cubic erbium film. Figure 5 shows micrographs obtained before and after oxidation. The oxidation process is accompanied by a

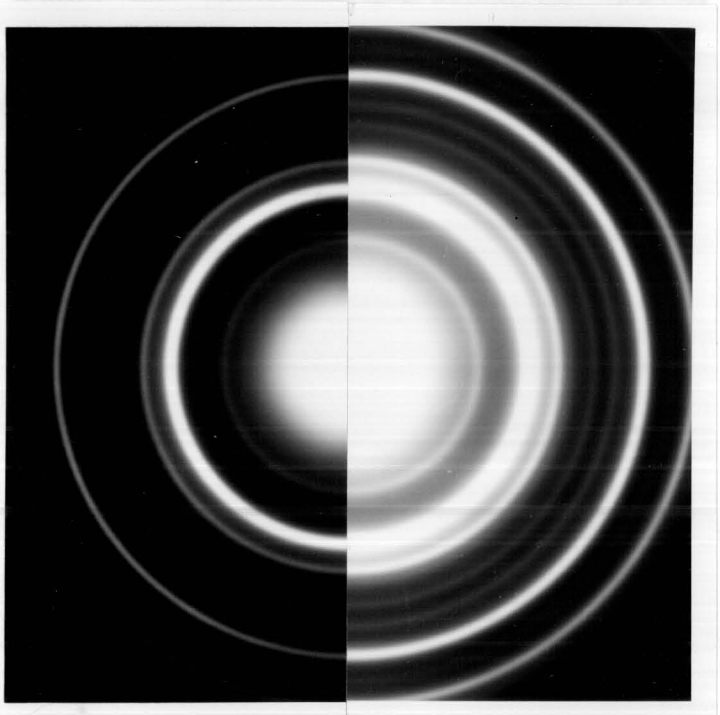

Figure 3: Electron diffraction pattern showing f.c.c. erbium and erbium oxide (Er_2O_3) contamination due to ungettered vacuum. 100 kV electrons.

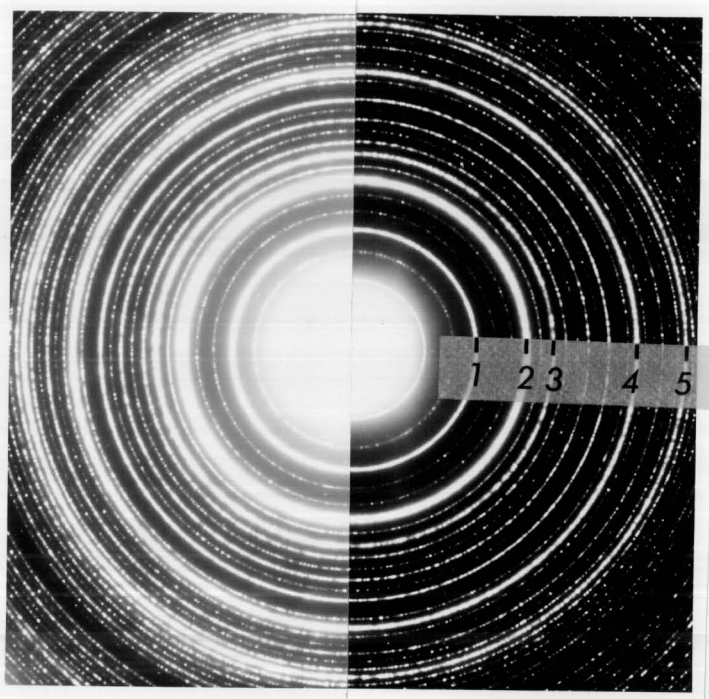

Figure 4: Cubic erbium oxide (Er_2O_3) produced by intense electron bombardment of a f.c.c. erbium film in the electron microscope. Rings 1,2,3,4 and 5 have the following indices: 211, 222, 400, 440, and 622, respectively.

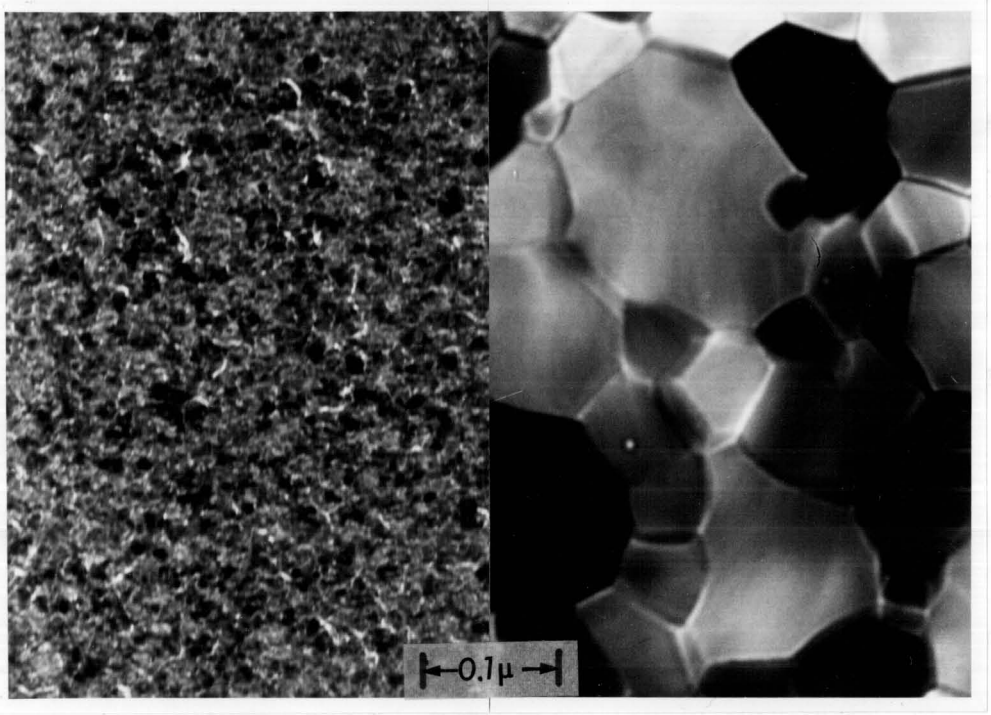

Figure 5: (a) Crystallites of f.c.c. erbium.

(b) Crystallites of erbium oxide (Er_2O_3) produced by intense electron bombardment of the erbium film shown in (a).

considerable increase in grain size. If the electron beam is kept at full intensity, the oxide crystals increase in size to such an extent that holes develop and the film eventually ruptures. Such an increase in grain size in thin films of Er_2O_3 was observed by Murr (1967) and is thought to be due to the thermal stresses in addition to the temperature rise set up by the pulse annealing effect of the electron beam (Singh and Srivastava, 1969). Thick films of the rare-earth metals under consideration possessing the normal h.c.p. structure behave in a similar manner with regard to oxidation. Table 3 gives the lattice parameters of the oxides produced by heating thin films of f.c.c. metal. The lattice parameters of these oxides which have a cubic crystal structure could be measured to about ½% because the diffraction patterns were extensive and the rings were sharp. The results agree well with those obtained by X-ray methods (Templeton and Dauben, 1954; Guth and Eyring, 1954).

The thicknesses at which the cubic form of the rare earth metals occur has not been studied with the exception of the case of erbium. By using the inverse square law and the mass of erbium evaporated to calculate the thickness it was found that a film about 140 Å thick contained only face-centred-cubic erbium whereas a film about 200 Å thick contained both the face-centred-cubic and hexagonal forms. Further studies involving thickness and the structure of erbium films were

Table 3: Lattice parameters in Å for rare-earth metal oxides. b_o are the parameters of the cubic oxides of the rare-earth metals observed in the present work; C_o are the lattice parameters of the cubic oxides of the rare-earth metals reported by Templeton and Dauben (1954) or by Guth and Eyring (1954).

Oxide	b_o	C_o
Gd_2O_3	10.80	10.81
Tb_2O_3	10.71	10.73
Dy_2O_3	10.62	10.67
Ho_2O_3	10.56	10.61
Er_2O_3	10.55	10.55
Tm_2O_3	10.46	10.49

conducted by means of a micro-balance. These are discussed below in more detail. It was also found in these studies that the hexagonal-close-packed form did not occur unless the films were about 200 Å or more thick. In thick films only hexagonal-close-packed erbium was observed. Though the thicknesses of films of the other metals was not known in Å the relative thicknesses of the films of a given metal could be estimated visually from their optical transmission. In all cases the face-centred-cubic form was observed in thin films and as film thickness increased so the hexagonal form became predominant.

The Philips E.M. 300 electron microscope used in the present studies is equipped with an evaporator which enables metals to be condensed on substrates inside the microscope (Curzon, 1971). In view of the reactivity of the rare-earth metals it was considered inadvisable to evaporate large quantities of the metals in the microscope, however, a few studies were made with erbium. It was found that in thin films the face-centred-cubic phase was observed and as the films became thicker so the normal hexagonal phase of bulk erbium became predominant, that is, the results were the same as those obtained for erbium films made in the vacuum coating unit and sandwiched between carbon films. All the metals studied were chemically similar hence the result for erbium also indicated that for the other metals the observation of face-centred-cubic

forms in thin films does not depend on whether the films are prepared in the electron microscope or a vacuum coating unit.

It has been suggested (Murr, 1973) that the face-centred-cubic electron diffraction pattern obtained in the present work (Curzon and Chlebek, 1972) from thin films formed by the evaporation of erbium was due to a metastable oxide ErO. A possible way to determine whether the face-centred-cubic phase was metallic erbium or ErO would be to oxidise a known weight of the material in air to Er_2O_3. When this technique was first tried problems of reproducibility were encountered. However, these problems have now been solved and it has been established beyond reasonable doubt that the face-centred-cubic phase is metallic erbium and not ErO. The experimental technique was as follows.

In a given experiment a thin glass microscope slide cover slip 1.8 cm square by 0.02 cm thick was heated in a propane flame in order to anneal it and thus reduce the risk of chipping during handling. The cover slip was then baked at 600°C for ten minutes in an electric furnace so that volatile contaminants could be removed in a controlled manner. The cover slip was supported on two ceramic rods and was surrounded by glass surfaces so as to minimize contamination of the slip by refractory dust particles from the lining of the furnace. After the slip had been weighed erbium was vapour deposited on its two surfaces in two successive depositions the thickness

being monitored by means of a Sloan quartz crystal thickness monitor. The erbium was evaporated from an electrically heated molybdenum spiral in a vacuum of 2×10^{-6} torr. The thickness deposited was of the order of 200 Å on each surface. The crystal structure of the films was checked by means of electron diffraction studies of specimens made by condensing erbium on thin carbon films placed close to the glass cover slip. In some cases a trace of the hexagonal-close-packed phase could be detected but in all cases the face-centred-cubic form was predominant.

The total weight of erbium deposited on a given cover slip was obtained by direct weighing with a Cahn micro-balance sensitive to 10^{-7} gram. The slip was then returned to the furnace and heated to 600°C for ten minutes. This caused the deposit which originally had a metallic lustre to become transparent due to the formation of Er_2O_3. The formation of this oxide was verified by electron diffraction experiments on thin films of carbon supported erbium deposits which were also baked at 600°C for ten minutes.

Table 4 lists not only the measured weight increases which occurred on oxidation to Er_2O_3 but also calculated weight increases assuming that the initial deposit was either erbium metal or ErO. Comparison of the measured and calculated increases in weight shows that the majority of the results agree with the assertion that the initial deposit formed by

Table 4: Weight increases in mgm of deposits vacuum condensed from erbium vapour and subsequently oxidised to Er_2O_3.

n = result index

W_1 = weight of the deposit before oxidation to Er_2O_3.

t = thickness of the deposit in Å calculated on the assumption that the deposit is Er.

W_2 = weight increase of the deposit due to oxidation to Er_2O_3.

W_3 = calculated weight increase assuming the deposit is Er.

W_4 = calculated weight increase assuming the deposit is ErO.

n	W_1	t	W_2	W_3	W_4
1	0.122	270	0.016	0.018	0.006
2	0.120	266	0.018	0.017	0.006
3	0.110	243	0.015	0.016	0.005
4	0.126	278	0.019	0.018	0.006
5	0.112	249	0.023	0.016	0.005
6	0.126	279	0.030	0.018	0.006
7	0.063	139	0.008	0.009	0.003
8	0.069	152	0.010	0.010	0.003
9	0.058	128	0.010	0.008	0.003
10	0.085	188	0.013	0.012	0.004
11	0.097	213	0.012	0.014	0.005
12	0.094	208	0.011	0.014	0.005
13	0.079	173	0.010	0.011	0.004
14	0.090	200	0.008	0.013	0.004
15	0.086	191	0.010	0.012	0.004
16	0.091	202	0.014	0.013	0.004
17	0.073	161	0.011	0.011	0.004
18	0.086	190	0.015	0.012	0.004
TOTAL:			0.253	0.242	.081

condensation of erbium vapour was erbium metal and not ErO. The reproducibility of the weights was tested by weighing a clean glass cover slip before and after heating it to 600°C for ten minutes and repeating this process several times for several different slips. This procedure was found to give weights reproducible to 0.003 mgm and this being so only result number 14 in table 4 could conceivably be used to support the view that the initial deposit was ErO. In order to reduce the error below 0.003 mgm it would probably be necessary to use a dust-free room and equipment. However, such complexity is not necessary; the present accuracy is sufficient to enable a decision to be made between the alternatives of erbium or ErO as the material of the initial deposit.

CHAPTER IV

DISCUSSION

IV-1 FACE-CENTRED-CUBIC Gd, Tb, Dy, Ho, Er and Tm

When a new phase is observed for a metal in the form of a thin film it is important to establish whether the material examined is the metal itself or whether it is a chemical compound which occurs because of contamination of the film. The films studied had metallic reflectivity, the low electrical resistance of metal films and transformed into oxides when heated in air or in a "vacuum" (10^{-5} torr) by an intense electron beam. All of these facts strongly suggest that the new phases were metallic. A further argument in favour of this conclusion is afforded by the thickness dependence of the structures of the films. As was stated earlier, condensation on a substrate was not allowed to begin until the gettering action had reduced the ambient pressure to a steady minimum. In this situation the rate of arrival of atoms of the metal being studied at the substrate was approximately constant as was the rate of arrival of atoms from contaminants in the vacuum. In thin films face-centred-cubic phases were observed whereas in thick films the normal hexagonal structures of the metals in bulk were observed. The measured lattice parameters of the hexagonal forms agreed within the experimental error of about 1% with X-ray results (Spedding and Beaudry,

1971) which indicates that in thick films the concentration of contaminants was not large enough to be detected. Since the thin films and the thick films were made in the same way and the thick films behaved as relatively uncontaminated metals it must be concluded that the face-centred-cubic phases observed in thin films were new phases of the metals and not compounds of the metals. Had they been compounds of the metals there is no reason why the same compounds should not have been seen in thicker films.

All the experimental results reported so far for Tb, Dy, Ho, Er and Tm are completely consistent with the suggestion that the face-centred-cubic phases which are associated with these metals are new forms of the metals. No result obtained for these phases requires an explanation in terms of a compound of a rare-earth metal and a contaminant in the vacuum such as oxygen or nitrogen. In the case of gadolinium there is some evidence to indicate that the films were contaminated with oxygen. Since the films possess marked metallic properties and strong electron diffraction rings from the usual oxide Gd_2O_3 were not observed it is reasonable to assume that even in this case the face-centred-cubic phase is characteristic of metallic gadolinium in thin films. There is evidence that recently a face-centred-cubic oxide GdO has been made by the vacuum distillation of a powder containing both Gd and Gd_2O_3 (Bist et al., 1972).

This GdO is thought to be formed by the reaction $Gd_2O_3 + Gd = 3\ GdO$ and its cubic structure has lattice parameter $a_o = 5.24 \pm 0.05$ Å which is not the same as $a_o = 5.40 \pm 0.05$ Å the lattice parameter of the face-centred-cubic phase produced in the present work by the evaporation of gadolinium metal. Although this face-centred-cubic phase may possibly be contaminated with some oxygen it is mainly gadolinium metal and not GdO.

IV-2. THE FACE-CENTRED-CUBIC PHASE FOR ERBIUM, Er or ErO?

In a recent letter Murr (1973) suggested that the face-centred-cubic electron diffraction pattern ($a_o = 5.09 \pm 0.05$ Å) obtained in the present work (Curzon and Chlebek, 1972) from thin films formed by the evaporation of erbium was due to a metastable oxide ErO and not to a new crystalline modification of metallic erbium which normally has the hexagonal-close-packed structure. The proposed oxide was used by Murr (1967) to account for a face-centred-cubic pattern which was observed in some regions of erbium films vapour-deposited on to (001) NaCl substrates. Murr (1967) prepared his erbium films by a pulse evaporation technique in an ultra high vacuum of 10^{-8} to 10^{-9} torr. That the vacuum during evaporation was worse than this is shown by the fact that mention is made of vacuum recovery between evaporations but no information is given concerning the pressure during evaporation. In the present

work the specimens were made in a vacuum of $\sim 10^{-6}$ torr during evaporation. Murr (1973) suggests that the difference in vacuum conditions for the two sets of experiments may account for the extensive occurrence of the face-centred-cubic phase in the present work.

In the following discussion it will first be pointed out that Murr's results are consistent with a face-centred-cubic form of erbium and then further evidence will be presented which shows that the results of the present experiments on erbium are not explicable in terms of the p-type semiconducting oxide ErO discussed by Murr.

Murr (1967) only observed the face-centred-cubic phase in localized regions of his erbium films. It is reasonable to suppose that the flux of any oxygen at the erbium film would be uniformly distributed over the substrate and hence the occurrence of localized regions of a face-centred-cubic oxide is unlikely especially as such regions would demand the diffusion of oxygen long distances over the reactive substrate. If it is assumed that the face-centred-cubic regions consisted of a new metastable form of metallic erbium then the occurrence of discrete areas of this material is easily explained. The cleavage face of NaCl contains cleavage steps and many other forms of defect which would act as preferred sites for the nucleation of the new form. The efficiency of nucleation is very sensitive to such defects hence an anisotropic distribution

of face-centred-cubic erbium embedded in hexagonal-close-packed erbium would be a distinct possibility. The face-centred-cubic form, since it is metastable, would presumably have a tendency to transform to the bulk hexagonal-close-packed form by the formation of stacking faults. Murr (1967) himself observed the extreme ease with which such faults developed. It could also be argued though perhaps less convincingly that the faults in the NaCl would generate defects in hexagonal-close-packed erbium and that these defects could act as preferred sites for the growth of face-centred-cubic ErO.

Murr (1973) suggests that the vacuum of 10^{-6} torr used during condensation of erbium films studied in the present experiments was sufficiently poor to lead to the formation of ErO. If this is so then other easily oxidizable metals such as thallium or zinc should also show evidence of oxidation when condensed in a similar vacuum. An experiment carried out on thallium showed that oxides of this metal were not observed when the metal was deposited in situ at about 10^{-5} torr inside the electron microscope but the metal rapidly oxidised when exposed to the atmosphere for a few seconds. Further evidence not considered by Murr which strongly argues against the interpretation involving ErO is the thickness dependence of the structures of the films already discussed in section IV-1 and the results of the weight increase measurements upon oxidizing

thin films of the f.c.c. phase to Er_2O_3 given in Chapter III.

The present work has shown that the face-centred-cubic phase had low electrical resistance. The conductivity of the erbium films has been measured, the thickness of the film being estimated from the geometry of the apparatus and the weight of erbium evaporated. The conductivity is of the order of 0.2×10^4 $(ohm\text{-}cm)^{-1}$ which compares with 0.12×10^5 $(ohm\text{-}cm)^{-1}$ for bulk erbium (Kittel, 1971, p. 260). The ratio of ~0.2 for these conductivities is to be expected because of defects in the thin films and surface effects. When films of the face-centred-cubic phase (coated with carbon to prevent them from being exposed to air) were cooled to 77°K the resistances changed by 0 to 10% which is certainly not consistent with the behaviour to be expected from the p-type semi-conducting film ErO proposed by Murr (1967) where the conductivity would change by at least an order of magnitude or more for an energy gap of reasonable size (say ~0.5 eV). On the other hand the fact that the conductivity did not change much agrees with the suggestion that the films studied were metallic, the conductivity being controlled by a large density of defects and surface effects.

Other metals are known which occur in both the hexagonal-close-packed and face-centred-cubic forms. For example thin films of face-centred-cubic β- cobalt (normally stable above 425°C) have been produced by electrodeposition onto face-

centred-cubic copper substrates (Goddard and Wright, 1964). Hence, it is not at all unreasonable to suppose that erbium could also occur in these two forms, especially since the face-centred-cubic form has about the same density as the hexagonal-close-packed form.

All the data so far obtained (the present work and Murr, 1967) may be easily explained in terms of a face-centred-cubic form of erbium which is only stable in thin films. Explanations based on a proposed face-centred-cubic ErO encounter various difficulties. These include: the oxide only occurs in thin films and occurs whether the vacuum is gettered with freshly condensed erbium or not; formation of the oxide in films of hexagonal-close-packed erbium was not observed (Er_2O_3 developed) in the work of Murr or in the present work and the "oxide" has an electrical conductivity which is characteristic of a metal instead of a p-type semiconductor. Also the weight increase on oxidation in air is consistent with the formation of Er_2O_3 from erbium and not from ErO.

IV-3 THICKNESS DEPENDENCE OF THE CRYSTAL STRUCTURE

As mentioned above thin films of many other materials have been observed which exhibit crystal structures which are different from the normal stable structures (Handbook of Thin Film Technology, 1970, pp. 10-45 to 10-52). Although the exact mechanism for the formation of the face-centred-cubic phase in thin films of the rare-earth metals under considera-

tion is not known some possible contributory factors will now be discussed.

Epitaxial effects may be ruled out since amorphous carbon films were used as substrates. However, the Ostwald rule (Chopra, 1969, p.199) according to which a system undergoing reaction proceeds from a less stable state to the final stable equilibrium state may be used to predict that the less stable f.c.c. phase is formed first during condensation. The f.c.c. and h.c.p. structure have the same numbers of nearest and next nearest neighbours hence the energy difference associated with the two phases is small and correspondingly the driving force for a phase transition is also small. From standard nucleation theory it follows that the probability of the formation of an h.c.p. nucleus decreases as the driving force decreases and increases as the specimen becomes thicker. This means that the h.c.p. phase would be expected to develop in relatively thick films as was in fact observed, the films being tens of interatomic distances thick ($\sim$200 Å). Another possible explanation of the dependence of crystal structure on thickness is that the stress between the substrate and the metal may stabilize the f.c.c. phase, an effect which becomes less important as the metal film increases in thickness.

IV-4 THE SPACE GROUP OF Er_2O_3. T_h^7 or T^5?

The crystal structure of Er_2O_3 has been reported in the past (Pauling and Shappell, 1930; Strukturbericht, 1928-32, p.38; Templeton and Dauben, 1954; Fert, 1962; Wyckoff, 1964, p.2) to be cubic with symmetry T_h^7(Ia3). However, Murr (1967)

when speaking of his electron diffraction patterns from Er_2O_3 states "the condition on Okℓ that k, (ℓ) = 2n (and cyclic) which is specific to the space group T_h^7 (Ia3) is violated by the prominent 200, 110, 220, etc. reflections observed (International Tables for X-ray Crystallography, 1969, Vol. 1, pp. 308 and 315) . . . ". In fact both 200 and 220 are allowed reflections for T_h^7 but 110 is forbidden. Murr deduces from his electron diffraction observations that the space group of Er_2O_3 is not T_h^7 but T^5 but fails completely to discuss the possibility that double diffraction in crystals having T_h^7 symmetry may be invoked to explain his results. It will now be shown that the electron diffraction evidence discussed by Murr is insufficient to establish which of the two space groups T_h^7 or T^5 is correct.

In the diffraction patterns from a polycrystalline cubic material the diffraction rings have radii proportional to $H = \sqrt{(h^2 + k^2 + \ell^2)}$. In the present work diffraction rings from Er_2O_3 with H^2 having values up to about 100 have been observed. Table 4 lists the hkℓ indices for forbidden rings of the type Okℓ in the space group T_h^7 where $H^2 \leq 100$. Also listed are the indices h'k'ℓ' of allowed rings which overlap forbidden rings. It is seen from the table that if Er_2O_3 has T_h^7 symmetry then three rings of the type Okℓ with the following indices should be absent, 110, 310, 730, since other

Table 5: $hk\ell$ = indices of forbidden rings of the type $Ok\ell$ in the space group T_h^7. $h'k'\ell'$ = indices of allowed rings in the space group T_h^7.
$H = \sqrt{(h^2+k^2+\ell^2)}$ or $\sqrt{(h'^2+k'^2+\ell'^2)}$.

h k ℓ	h'k'ℓ'	H^2
110		2
310		10
330	411	18
510	431	26
530	433	34
550	543	50
710	543	50
730		58
750	743	74
770	941	98
910	833	82
930	754	90

allowed rings will not overlap these forbidden rings. These rings are in fact observed in the diffraction patterns from Er_2O_3 (the present work and Murr, 1967) though the 730 ring is very weak. At the same time the 112, 222, and 622 rings are strong. It is conceivable that the forbidden reflections 110, 310, 730 appear not because the T_h^7 space group is incorrect for Er_2O_3 but because double diffraction leads to the appearance of these reflections according to the relations

$$110 = 222 + \bar{1}\bar{1}\bar{2}$$

$$310 = 222 + 1\bar{1}\bar{2}$$

$$730 = 622 + 11\bar{2}$$

where the reflections on the right in the above equations are all allowed in T_h^7. X-ray measurements, for which double diffraction is little problem, carried out on Er_2O_3 by the National Bureau of Standards (1956) and quoted by Murr (1967) are consistent with the space group T_h^7 and inconsistent with T^5. In this work (National Bureau of Standards, 1956) some rings are observed which appear to violate the condition on $Ok\ell$ that k, (ℓ) = 2n but the violation is only apparent and is due to overlap by allowed rings (see Table 5). The present work and that of Murr (1967) was carried out on films ~200 Å or more in thickness which is too thick for kinematic electron diffraction theory to be applicable. Hence the above explanation based on double diffraction and used to account for the

appearance of the forbidden reflections 110, 310, 730 in T_h^7 is reasonable. In order to use electron diffraction to show that the space group of Er_2O_3 is not T_h^7 but T^5 (for which the 110, 310 and 730 reflections are allowed) it would be necessary either to study much thinner films of oxide in which the kinematic approximation could be used or alternatively single crystals mounted in a tilting holder could be studied, dark field and selected area techniques being used to check that double diffraction was absent. However such work is not necessary because the X-ray studies have ruled out T^5 as a possible space group for Er_2O_3.

IV-5. THE OXIDATION OF F.C.C. ERBIUM

The relation of f.c.c. erbium to the oxide is of interest and will now be discussed. As stated above Er_2O_3 has a cubic crystal structure with symmetry T_h^7 (International Tables for X-ray Crystallography, 1969, Vol. 1, pp. 315 and 498). The lattice parameter is 10.55 Å. There are 8 erbium atoms in the b positions and 48 in the e positions with $x_{Er} = -0.0330 \pm 0.0006$ (Fert, 1962), and 24 oxygen atoms in the d positions with $x_o = 0.394 \pm 0.001$, $y_o = 0.149 \pm 0.001$ and $x_o = 0.380 \pm 0.001$. When, for simplicity, x_{Er} is taken to be zero it turns out that the erbium atoms form a face-centred-cubic lattice with a lattice parameter of 5.28 Å which is half that

of the oxide. This is shown schematically in figure 6. The lattice parameter of the cubic form of erbium is 5.09 Å; thus, when the cubic form of erbium is oxidised to Er_2O_3, the separation of the erbium atoms increases by the small amount of ~ 4%. There is also slight rearrangement of the erbium atoms corresponding to the fact that x_{Er} is not exactly zero.

The curious fact that rings 2-5 of figure 4 have approximately the same radii as corresponding rings in figure 1 is explained as follows. Rings 2-5 are due in large part to erbium atoms with small contributions from oxygen atoms which scatter electrons much less strongly than the erbium atoms. Figure 1 is due entirely to erbium atoms. Since the erbium atoms in both the oxide and the metal are on very similar lattices, it follows that rings 2-5 should correspond closely to rings produced by the pure metal as is, in fact, the case. The prominent 211 ring of figure 4 is due almost entirely to oxygen atoms.

- A discussion of the oxidation of the cubic forms of the other metals under investigation would be similar to that for erbium and hence is omitted.

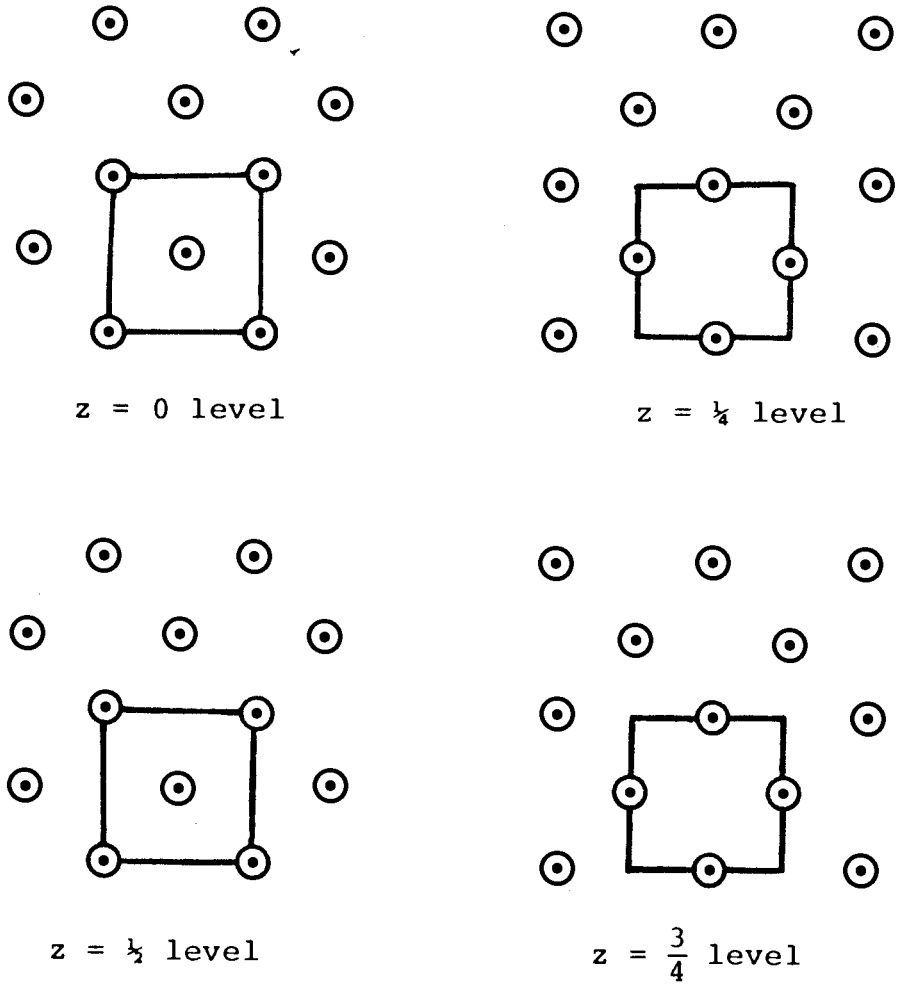

Figure 6: Positions of the erbium atoms in Er_2O_3 taking $x_{Er} = 0$ for simplicity. The erbium atoms form a f.c.c. lattice with a lattice parameter equal to one half that of the oxide lattice parameter.

IV-6. A COMMENT ON THE VALIDITY OF RECENT ELECTRON MICROSCOPE OBSERVATIONS OF GADOLINIUM MONOXIDE AND A RELATED LOWER OXIDE

A number of papers (Rai and Srivastava, 1971, Bist and Srivastava, 1971; Bist et al., 1972) have recently appeared which report the results of electron microscope and diffraction studies on gadolinium monoxide and suboxide of the form $GdO_{0.656}$. The validity of the interpretation of the experimental results is discussed below in terms of the electron microscope and diffraction studies carried out in the present work on thin films of rare-earth metals.

Rai and Srivastava (1971) have reported that single crystals of GdO are obtained when the vapour of 99.95% pure gadolinium is condensed on the 100 face of freshly cleaved NaCl, the temperature of the NaCl being 550°C and the vacuum being about 10^{-5} torr. The deposit of GdO so obtained was reported to have an NaCl-type face-centred-cubic lattice with a spacing of 5.50 ± 0.03 Å. In later work (Bist and Srivastava, 1971; Bist et al., 1972) GdO was prepared by vacuum distillation at about 1800°C in a vacuum of 10^{-6} torr of a powder containing both Gd_2O_3 and Gd. This deposit of GdO had a zinc sulphide type face-centred-cubic structure with a lattice parameter of 5.24 ± 0.05 Å. In view of the different crystal structures and lattice parameters reported for the

deposits formed during the two different methods of preparation it appears unlikely that both materials were GdO, thus it is necessary to discuss whether one of the deposits could have been a material other than GdO.

It has been argued above that face-centred-cubic gadolinium metal has been prepared in the present work by condensation of gadolinium vapour. The lattice parameter of this phase is $a_o = 5.40 \pm 0.05$ Å which compares with the parameter of $a_o = 5.50 \pm 0.03$ Å obtained for the cubic phase reported by Rai and Srivastava (1971). It thus appears that the cubic phase obtained by vapour deposition of gadolinium on rock-salt (Rai and Srivastava, 1971) may have been metallic face-centred-cubic gadolinium and not NaCl type face-centred-cubic GdO as reported.

The phase obtained by distillation of a powder containing Gd and Gd_2O_3 was shown to be GdO by means of the weight gain which occurred when the phase was oxidized in air to Gd_2O_3 (Bist et al., 1972). A similar test has not been carried out for the deposit formed when the vapour from gadolinium alone is condensed.

When in the present work face-centred-cubic gadolinium or normal hexagonal-close-packed gadolinium was pulse annealed inside the electron microscope a diffraction pattern which could be interpreted entirely in terms of Gd_2O_3 was obtained. The measured lattice parameter was 10.80 ± 0.05 Å which

compares with the X-ray value of 10.813 Å (Templeton and Dauben, 1954). Some weak "forbidden" rings were observed in the electron diffraction patterns but they are explicable in terms of the double diffraction which frequently occurs in electron diffraction studies and for which a detailed discussion was given in section IV-3 for the case of Er_2O_3. It is interesting to note that erbium oxidized more readily than gadolinium. Erbium could be oxidized by illuminating it with an intense electron beam but with the apertures of the condenser lenses still in position. In order to oxidize the gadolinium both apertures of the condenser lenses had to be removed. Bist et al., (1972) found that gadolinium did not oxidize at an appreciable rate in air until the temperature exceeded 750°C. This being so, it appears that even when gadolinium is deposited in a vacuum of 10^{-5} torr on to a substrate of 550°C it should not oxidize appreciably. This conclusion reinforces the view expressed earlier that Rai and Srivastava (1971) observed not GdO but metallic gadolinium when they condensed gadolinium vapour on NaCl.

When Rai and Srivastava (1971) pulse annealed the films they obtained by condensing gadolinium vapour on NaCl they observed the formation of a cubic super lattice with lattice parameter $a_o = 10.90 \pm 0.09$ Å. This result is consistent with the accepted lattice parameter of $a_o = 10.813$ Å for

Gd_2O_3 (Templeton and Dauben, 1954), but the superlattice was of face-centred-cubic type which does not agree with the T_h^7 symmetry of Gd_2O_3 (Strukturbericht, 1928-32). Rai and Srivastava (1971) suggest that the phase in question develops because pulse annealing leads to loss of oxygen from the initial material which was thought to be GdO. As pointed out earlier this initial material was probably gadolinium and not GdO but even assuming the initial material were GdO the suggested mechanism for the development of the superlattice is at variance with results obtained in the present work. Both hexagonal-close-packed and face-centred-cubic gadolinium oxidize to Gd_2O_3 when subjected to pulse annealing. This means that GdO when pulse annealed would be expected to oxidize further instead of losing oxygen as Rai and Srivastava suggested. It is clear that further work is required in order to establish the nature of the superlattice. In particular its chemical composition should be determined by noting any increase of weight which occurs when the material is heated in air. In view of the closeness of the lattice parameter to that of Gd_2O_3 it is conceivable that the superlattice is a non-stoichiometric form of Gd_2O_3 in which vacancies are ordered.

Bist et al., (1971, 1972) have shown that GdO may be made by vacuum distillation of a powder containing both gadolinium metal and Gd_2O_3. When GdO is pulse annealed it is reported that $GdO_{0.656}$ forms, that is, pulse annealing leads to a

reduction of GdO (Bist et al., 1972). It is known that pulse annealing of some oxides such as MoO_3 leads to their reduction (Bursill, 1969) but as has just been stated the present studies on the oxidation of metallic gadolinium to Gd_2O_3 indicate that pulse annealing of GdO should lead to its oxidation and not its reduction. The formula $GdO_{0.656}$ is based entirely on electron diffraction studies. The question therefore arises as to whether the analysis of these studies is correct. Electron diffraction studies can be used to obtain accurate information about the geometry of unit cells but is very unreliable with regard to atomic positions particularly for the films studied by Bist et al., which had an average thickness of 500 Å. In such relatively thick films dynamical interactions can be very strong. Bist et al., pointed this fact out but proceeded to use their intensity data to determine the contents of the unit cell of $GdO_{0.656}$. As will be discussed below, the electron diffraction studies of Bist et al., are not sufficient in themselves to justify the existence and proposed crystal structure of the oxide $GdO_{0.656}$.

The pulse annealing of GdO made by vacuum distillation of a powder containing gadolinium metal and Gd_2O_3 (Bist and Srivastava, 1971; Bist et al., 1972) reportedly leads to the formation of a superlattice with rhombohedral symmetry, the hexagonal axes of the unit cell of the superlattice being

$a = 2\sqrt{2}\ a_o$ and $c = 2\sqrt{3}\ a_o$ where $a_o = 5.24 \pm 0.05$ Å is the lattice parameter of GdO. The c/a ratio of $\sqrt{3}/\sqrt{2}$ corresponds to a simple cubic unit cell with a lattice parameter in the present case of $b_o = 2a_o = 10.48$ Å (International Tables for X-ray Crystallography, 1969, Vol. 2, p. 154) thus the positions of the superlattice spots in the diffraction patterns reported by Bist et al., can be interpreted in terms of a cubic unit cell. This does not of course imply that the superlattice necessarily has cubic symmetry. The superlattice (Bist and Srivastava, 1971; Bist et al., 1972) has been interpreted in terms of an ordered array of oxygen atoms in a lattice of rhombohedral symmetry, the chemical formula of the compound being $GdO_{0.656}$. Bist et al., (1972) point out that the gadolinium atoms in rhombohedral $GdO_{0.656}$ lie on a face-centred-cubic lattice. It is worthy of note that the oxygen atoms lead to a decrease of lattice symmetry from cubic to rhombohedral and yet at the same time the symmetry of the metal atoms is cubic and also a cubic shaped unit cell with its axes parallel to the cube axes of the metal lattice can be used to describe $GdO_{0.656}$. Such a situation is of course possible in principle but the cubic symmetry of the metal atoms and the cubic shape of the unit cell suggest that a possible cubic symmetry of the entire lattice (gadolinium plus oxygen) should be examined. Bist et al., rejected cubic symmetry because of the geometries of their observed superlattice

patterns and referred in support of this rejection to a diffraction pattern showing a {211} section through the GdO reciprocal lattice. If allowance is made for the fact that the electron beam is not exactly along the GdO [211] direction it becomes apparent that the GdO and superlattice spots in the published pattern have mirror symmetry about the GdO - $[\bar{1}11]$ and $[01\bar{1}]$ lines of spots. Such symmetry is consistent with the cubic point group m3m (International Tables for X-ray Crystallography, 1969, Vol. 1, pp. 27 and 30), thus Bist et al., are mistaken in asserting that their published [211] diffraction pattern supports their view that the reported superlattice is not cubic. It may be the case that their assertion is correct but this cannot be ascertained until a diffraction pattern is presented which definitely contradicts m3m. Two other diffraction patterns of the superlattice of GdO have also been published. One of these is a {111} GdO reciprocal lattice section which has six-fold rotation symmetry. Such symmetry is consistent with cubic, rhombohedral or hexagonal symmetry. The remaining published diffraction pattern is a {123} GdO reciprocal lattice section. This pattern contains a $\{\bar{1}\bar{1}1\}$ axis which is a three-fold inversion axis in m3m. Assuming that the $[\bar{1}\bar{1}1]$ axis is in fact a three-fold inversion axis then inversion symmetry would be expected in the {123} section. Such symmetry is however

always observed for diffraction patterns where resonance effects can be neglected (International Tables for X-ray Crystallography, 1969, Vol. 1, pp. 27 and 30) hence the {123} diffraction pattern does not give symmetry information which is of use in determining whether the superlattice of GdO is cubic or not. The facts that the published diffraction patterns from the superlattice are consistent with cubic symmetry and that the positions of the diffraction spots are given by a cubic unit cell argue against the interpretation by Bist et al., in terms of a lattice of rhombohedral symmetry. In addition, as pointed out previously, the oxidation to Gd_2O_3 which occurs when gadolinium is pulse annealed shows that the pulse annealing of GdO would be expected to lead to a higher oxide and not to the lower oxide $GdO_{0.656}$ proposed by Bist et al., (1972). Dynamical interaction in films 500 Å thick such as were used by Bist et al., is likely to be so strong that intensity measurements would be totally unreliable. This being so, electron diffraction studies of such films should be mainly restricted to the determination of the size and shape of a unit cell. The determination of unit cell contents is likely to be unreliable. At the very least a proposed structure such as $GdO_{0.656}$ should be confirmed by a study of the weight increase which occurs when the film is heated in air to form Gd_2O_3. With the evidence presently available it is highly likely that the superlattice

obtained by pulse annealing GdO is not $GdO_{0.656}$ but is in fact an oxide containing more oxygen than GdO.

LIST OF REFERENCES

PART A

Boersch, H., Bostanjoglo, O. and Lischke, B., 1966/1967. Optik, 24, 460-5.

Cotterill, R. M. J., 1964. Proc. 3rd European Reg. Conf. Electron Microscopy, Prague, 63-4.

Curzon, A. E. and Pawlowicz, A. T., 1965. Proc. Phys. Soc., 85, 375-81.

Curzon, A. E., 1969. Micron, 1, 326-38.

Curzon, A. E., 1970. Canadian J. Phys., 48, 2852-6.

Honig, R. E. and Hook, H. O., 1960. R.C.A. Rev., 21, 360-8.

Kitamura, N., Srivastava, O. N., and Silcox J., 1966. 6th Int. Congr. Electron Microscopy, Kyoto (Tokyo: Maruzen), 1, 169-70.

Piercy, G. R., Gilbert, R. W. and Howe, L. M., 1963. J. Sci. Instrum., 40, 487-9.

Valdrè, U. and Goringe, M. J., 1965. J. Sci. Instrum., 42, 268-9.

Valdre, U. and Goringe, M. J., 1970. J. Phys. E: Sci. Instrum., 3, 336-7.

Venables, J. A., 1963. Rev. Sci. Instrum., 34, 582-3.

Venables, J. A., Ball, D. J. and Thomas, G. J., 1968. J. Phys. E: Sci. Instrum., 1, 121-6.

Watanabe, Hiroshi, 1965. Japan.J. Appl. Phys., 4, 384-5.

Watanabe, Hiroshi and Ishikawa, Isao, 1967. Japan.J. Appl. Phys., 6, 83-8.

PART B

Bist, B. M. S., Kumar, J. and Srivastava, O. N., 1972. Phys. Status Solidi (A), 14, 197-206.

Bist, B. M. S. and Srivastava, O. H., 1971. Phys. Status Solidi (A), 7, K9-K11.

Bursill, L. A., 1969. Proc. Roy. Soc., A311, 267-90.

Chopra, K. L., 1969. Thin Film Phenomena, McGraw-Hill Book Co., New York.

Curzon, A. E., 1971. Rev. Sci. Instrum., 42, 545-6.

Curzon, A. E. and Chlebek, H. G., 1972. J. Less-Common Metals, 27, 411-5.

Fert, A., 1962. Bull. Soc. Fr. Miner. Cryst., 85, 267-70.

Goddard, J. and Wright, J. G., 1964. Brit. J. Appl. Phys., 15, 807-14.

Guth, D. E. and Eyring, L., 1954. J. Am. Chem. Soc., 76, 5242-4.

Handbook of Thin Film Technology, 1970. Maissel, L. I. and Glang, Reinhard (eds.), McGraw-Hill Book Co., New York.

Hirsch, P. B., Howie, A., Nicholson, R. B., Pashley, D. W. and Whelan, M. J., 1965. Electron Microscopy of Thin Crystals, Butterworths, Washington.

International Tables for X-ray Crystallography, 1969, Vols. 1 and 2. Henry, N. F. M. and Lonsdale, K. (eds.), Kynoch Press, England.

Kittel, C., 1971. Introduction to Solid State Physics, John Wiley & Sons, Inc., New York, Fourth Edition.

Murr, L. E., 1967. Phys. Status Solidi, 24, 135-48.

Murr, L. E., 1973. J. Less-Common Metals, 30, 321-2.

National Bureau of Standards (U.S.A.), Circular No. 529, Vol. 8, 1956, 25-7.

Pauling, L. and Shappell, M. D., 1930. Z. Krist., 75, 128-42.

Rai, K. N. and Srivastava, O. N., 1971. Mater.Sci. Eng., 8, 341-2.

Singh, H. P. and Srivastava, O. N., 1969. Scripta Metallurgica, 3, 143-4.

Spedding, F. H. and Beaudry, B. J., 1971. J. Less-Common Metals, 25, 61-73.

Strukturbericht, 1928-32, Vol. 2.

Templeton, D. H. and Dauben, C. H., 1954. J. Am. Chem. Soc., 76, 5237-9.

Wyckoff, R. W. G., 1964. Crystal Structures, Vol. 2, John Wiley & Sons, Inc., Second Edition.